

Weighted Optimization: better generalization by smoother interpolation

Yuege Xie^{*} Rachel Ward^{* †} Holger Rauhut[‡] Hung-Hsu Chou[‡]

Abstract

We provide a rigorous analysis of how implicit bias towards smooth interpolations leads to low generalization error in the overparameterized setting. We provide the first case study of this connection through a random Fourier series model and weighted least squares. We then argue through this model and numerical experiments that normalization methods in deep learning such as weight normalization improve generalization in overparameterized neural networks by implicitly encouraging smooth interpolants.

1 Introduction

Consider the following regression/interpolation problem: we have n training data $(\mathbf{x}_j, y_j) \in \mathcal{D} \times \mathbb{C}$ corresponding to samples of an unknown function $y_j = f(\mathbf{x}_j)$ and the sampling points are drawn from the domain $\mathcal{D} \subset \mathbb{R}^d$. We fit the data with a hypothesis class $\mathcal{H} := \{f_{\boldsymbol{\theta}}(\mathbf{x}) : \mathbb{R}^d \rightarrow \mathbb{C}, \boldsymbol{\theta} \in \mathbb{R}^p\}$ by solving for a set of parameters minimizing the empirical ℓ_2 -risk

$$\boldsymbol{\theta}_{opt} \in \arg \min_{\boldsymbol{\theta} \in \mathbb{R}^p} \sum_{j=1}^n |f_{\boldsymbol{\theta}}(\mathbf{x}_j) - y_j|^2. \quad (1)$$

Traditionally, the number of parameters p is restricted to be smaller than the number of training samples, i.e., $p \leq n$, to avoid overfitting. For $p > n$, the solution $\boldsymbol{\theta}_{opt}$ is often not unique and traditional wisdom says that explicit regularization such as weight decay must be added to ensure that the solution is stable or meaningful. However, such wisdom has been challenged by modern machine learning practice, where small generalization error is achieved with massively *overparameterized* ($p \gg n$) hypothesis classes \mathcal{H} such as deep neural networks, without any explicit regularization. This implies that in such settings, the optimization method used for (1) has a favorable *implicit* bias towards a particular choice of $\boldsymbol{\theta}_{opt} \in \mathcal{H}$ among all empirical risk minimizers. As neural networks can be trained with a particularly simple algorithm, (stochastic) gradient descent, a flurry of research in the past several years, starting with Simonyan and Zisserman (2014); He et al. (2015); Zhang et al. (2016); Canziani et al. (2016), has been devoted to answering the question:

How and in what situations does the implicit bias of gradient descent interact favorably with the structure of a particular learning problem to achieve better performance in the interpolation regime?

The papers Belkin et al. (2018) and Liang and Rakhlin (2018) were first to observe that the power of overparameterization is not limited to neural networks, and can be found in *linear* interpolation models, where the feature basis $\{\psi_k\}_{k=1}^p$ is fixed and the empirical risk is a quadratic function of the parameters: $\sum_{j=1}^n (\sum_{k=1}^p \theta_k \psi_k(\mathbf{x}_j) - y_j)^2 = \|\Psi\boldsymbol{\theta} - \mathbf{y}\|^2$. In this setting, the implicit bias of gradient descent is well understood: by applying (stochastic) gradient descent to the empirical loss

^{*}Oden Institute, University of Texas at Austin. Email: yuege@oden.utexas.edu

[†]Mathematics Department, University of Texas at Austin.

[‡]Chair for Mathematics of Information Processing, RWTH Aachen University.

(1) with initialization belonging to the range of the feature matrix Ψ , the solution converges to the parameter solution θ_{\min} of minimal ℓ_2 -norm among all interpolating solutions.⁴

The seminal work Belkin et al. (2019a) claimed that improvement in generalization error is due to the connection between small ℓ_2 -norm of a parameter solution θ_{opt} and *smoothness* of the corresponding interpolating function $f_{\theta_{opt}}$. This connection was highlighted through the example of linear interpolation with random Fourier features (Rahimi and Recht, 2008) where the features basis $\psi_k : \mathbb{R}^d \rightarrow \mathbb{C}$ are random complex exponentials $\psi_k(\mathbf{x}) = e^{i\langle \mathbf{w}_k, \mathbf{x} \rangle}$ with $\mathbf{w}_k \sim \mathcal{N}(\mathbf{0}, \mathbf{I}_d)$, and which can be viewed as a class of two-layer neural networks with fixed weights in the first layer. As the number of random features $p \rightarrow \infty$, this basis converges to that of the reproducing kernel Hilbert space (RKHS) of smooth functions corresponding to the Gaussian kernel, and the interpolating solution found by gradient descent converges to the smooth function with minimal RKHS norm.

However, while this connection between minimal ℓ_2 -norm and smoothness of the solution is intriguing, *a rigorous analysis of how implicit bias towards smooth interpolations leads to low generalization error in the overparameterized setting* still remains. In this paper, we initiate this analysis by deriving exact expressions for the generalization error in a Fourier series model, and show precisely how an implicit bias towards smooth interpolants, in the form of weighted optimization, results in smaller generalization error in the overparameterized regime compared to the underparameterized regime. Beyond the Fourier series model, we connect weighted optimization to normalization methods in modern machine learning such as weight normalization, and we conclude that an implicit bias towards smoother solutions explains the good performance of such normalization in practice.

Contributions of this work. We consider the method of weighted ℓ_2 -norm interpolation in Fourier feature space, where the weight on a particular feature is proportional to the q th power of its gradient norm to encourage lower-frequency features. This additional degree of freedom, which is possible only in the overparameterized regime, enables us to reduce the risk. Remarkably, we show that under certain circumstances, the solution in the overparameterized regime is strictly better than that in the underparameterized regime, providing insight into the power of overparameterization in modern machine learning.

Formally speaking, we consider the feature space of Fourier series basis functions $\psi_k = e^{ixk}$ up to degree $|k| \leq p$, and the class of functions on the circle with sharply decaying Fourier series, where the decay rate corresponds to their smoothness. With n equispaced training evaluations of such a function, we provide an exact expression for the risk of weighted ℓ_2 -norm interpolation as a function of the number of features p , the number of samples n , the rate of decay r in the Fourier series of the underlying function, and the choice of weight q in the reparameterized ℓ_2 interpolation.

Our key theoretical results for weighted feature interpolation are as follows. For fixed number of samples n and number of features p : (a) For $q \geq r \geq 1$, the minimal risk in the overparameterized regime is strictly less than the minimal risk in the underparameterized regime; (b) For $q = r > 1/2$ and for any $p \geq n$, the risk for weighted interpolation is at most $\mathcal{O}(n^{-2r+1})$, and for large n, p, D , $\text{risk}_q \lesssim 2n^{-2r+1} + \frac{2}{2r-1}(2n)^{-2r}p^{-2r+1}$.

Weighted ℓ_2 interpolation can lose its advantage as we go to higher-dimensional domains $\mathcal{D} \subset \mathbb{R}^d$ where, for example, the random Fourier features $e^{i\langle \mathbf{w}_k, \mathbf{x} \rangle}$ will have comparable gradient norms by concentration of measure. However, it is sensible to consider weighted optimization (WO) for two-layer neural networks where the $\mathbf{w}_k \in \mathbb{R}^d$ become free parameters to optimize. In fact, we show that the resulting weighted optimization algorithm corresponds precisely to the well-known *weight normalization* (WN) algorithm (Salimans and Kingma, 2016) with fixed scale parameters g , which was introduced as a simple alternative to *batch normalization* (Ioffe and Szegedy, 2015), which is widely used for its remarkable and still mysterious ability to reduce generalization error in overparameterized neural networks. Moreover, we show that our weighted optimization algorithm performs comparably to weight normalization on several large-scale learning problems. Thus, we hypothesize that the scale parameter g in weight normalization is of secondary importance compared to the directional parameters, and more broadly that weight normalization and batch normalization achieve lower generalization error in part due to their underlying implicit bias towards smoother interpolants. We acknowledge that connection between batch normalization and smoothness has been

⁴Observe that the gradient descent iterates θ_t remain in the row span of the feature matrix Ψ if θ_0 is in the row span, and the minimal-norm solution is the unique solution in the row span of the feature matrix in the overparameterized setting.

made previously Santurkar et al. (2018), but with a focus on its connection to accelerated training rather than generalization error.

Previous work on generalization and overparameterization. The work of Belkin et al. (2019a) initiated the study of the extended bias-variance trade-off curve, and showed that double descent behavior is often exhibited, where the risk in the overparameterized regime $p \gg n$ can decrease to a point below the best possible risk in the underparameterized regime. They illustrated that this behavior occurs also in kernel regression/interpolation problems.

Subsequently, several works derived quantitative bounds on the risk in the interpolating setting, but required that either (a) the features are random (so that random matrix theory can be leveraged) or (b) p and n are in the asymptotic regime and go to infinity at a comparable rate. In contrast, our results are for deterministic Fourier features and hold for any p and n . Hastie et al. (2019) derived the precise high-dimensional asymptotic risk, for a general random model with correlated covariates. The work Bartlett et al. (2020) derived sharp bounds on the risk in general linear regression problems with non-isotropic subgaussian covariates, and highlighted the importance of selecting features according to the higher-variance covariates. Other works in this direction include Ghorbani et al. (2019); Mei and Montanari (2019); Geiger et al. (2020); Nakkiran et al. (2019).

Prior to the above line of works, Belkin et al. (2019b)—which was a large inspiration for us—considered the discrete Fourier series model we consider, but with a theoretical analysis only for randomly chosen Fourier features, unweighted optimization, and isotropic covariates, in the asymptotic setting. Empirical evidence pointing to improved generalization using weighted optimization and truncated Fourier series instead of random Fourier frequencies was provided, but without theoretical analysis. In this sense, our paper can be viewed as answering an open question regarding the role of weighted optimization in Fourier series interpolation from Belkin et al. (2019b).

2 Weighted optimization, random Fourier series and smooth interpolation

Smooth functions are characterized by the rate of decay in their Fourier series coefficients—the smoother the function, the faster the decay.⁵ Drawing inspiration from this connection, we consider as a model for random smooth periodic functions the class of trigonometric polynomials $f : [-\pi, \pi] \rightarrow \mathbb{C}$ with random r -decaying Fourier series coefficients:

Definition 2.1. (Random Fourier series with r -decaying coefficients) Fix $D \in \mathbb{N}$ and $r \geq 0$. We say that a function is a random Fourier series with r -decaying coefficients if⁶

$$f_{\boldsymbol{\theta}}(x) = \sum_{k=0}^{D-1} \theta_k e^{ikx}, \quad 0 \leq x \leq 2\pi, \quad (2)$$

where $\boldsymbol{\theta} \in \mathbb{C}^D$ is a random vector satisfying $\mathbb{E}[\boldsymbol{\theta}] = \mathbf{0}$ and

$$\mathbb{E}[\boldsymbol{\theta}\boldsymbol{\theta}^*] = c_r \Sigma^{2r} \quad \text{where } \Sigma := \text{diag}((k+1)^{-1}, k=0, 1, \dots, D-1) \in \mathbb{R}^{D \times D}, \quad (3)$$

and $c_r = \left(\sum_{k=0}^{D-1} (k+1)^{-2r}\right)^{-1}$ so that $\mathbb{E}[\|\boldsymbol{\theta}\|^2] = 1$.

We observe $n \leq D$ training samples $(x_j, y_j)_{j=0}^{n-1} = (x_j, f_{\boldsymbol{\theta}}(x_j))_{j=0}^{n-1}$ of such a function $f_{\boldsymbol{\theta}}$ at equispaced points on the domain, $x_j = \frac{2\pi j}{n}$, $j \in [n]$, where $[n]$ denotes the set $\{0, \dots, n-1\}$ for notation simplicity.

⁵the classical Sobolev spaces are Hilbert spaces defined in terms of Fourier series whose coefficients decay sufficiently rapidly. For square-integrable complex-valued functions f on the circle \mathbb{T} , consider the space of functions $H^r(\mathbb{T}) = \{f \in L^2(\mathbb{T}) : \|f\|_{r,2}^2 := \sum_{j=-\infty}^{\infty} (1+|j|^2)^r |\hat{f}(j)|^2 < \infty\}$, $r \in \mathbb{R}, r \geq 0$, where $\hat{f}(j)$ is the j th Fourier series coefficient of f . If $r \in \mathbb{N}$ then by duality between differentiation in time and multiplication in frequency, the Sobolev norm is equivalently defined in terms of the r th derivative $f^{(r)}$: $\|f\|_{r,2}^2 = \|f\|_{L_2}^2 + \|f^{(r)}\|_{L_2}^2$.

⁶For ease of exposition we only work with positive frequencies, although it may seem more natural to work with trigonometric polynomials of the form $f(x) = \sum_{k=-D}^D \theta_k e^{ikx}$. All our results can also be formulated within that setting, by symmetrically extending the weights to negative indices k and by replacing D with $2D-1$, and similarly for n and p below. The notation, however, will become more heavy then and comparison with other works less straightforward.

We can express the observation vector $\mathbf{y} \in \mathbb{C}^n$ concisely as $\mathbf{y} = \mathbf{F}\boldsymbol{\theta}$ in terms of the *sample discrete Fourier matrix* $\mathbf{F} \in \mathbb{C}^{n \times D}$ whose entries are $(\mathbf{F})_{j,k} = e^{ikx_j} = e^{2\pi ijk/n}$, $j \in [n]$, $k \in [D]$. If D is a multiple of n , i.e., $D = \tau n$ for $\tau \in \mathbb{N}$, then we can write $\mathbf{F} = [\mathbf{F}^{(n)} | \mathbf{F}^{(n)} | \dots | \mathbf{F}^{(n)}]$, where $\mathbf{F}^{(n)} \in \mathbb{C}^{n \times n}$ is the discrete Fourier matrix in dimension n .

We fit the training samples to a degree- p trigonometric polynomial $f_{\hat{\boldsymbol{\theta}}}(x) = \sum_{k=0}^{p-1} \hat{\theta}_k e^{ikx}$ such that $\hat{f}_{\hat{\boldsymbol{\theta}}}(x_j) \approx f_{\boldsymbol{\theta}}(x_j)$, $j \in [n]$, i.e., $\mathbf{y} \approx \mathbf{F}_T \hat{\boldsymbol{\theta}}$, where $\mathbf{F}_T \in \mathbb{C}^{n \times p}$ is the matrix containing the first p columns of \mathbf{F} , indexed by $T = [p]$. We solve for $\hat{\boldsymbol{\theta}}$ as the least squares fitting vector in the regression regime $p < n$, and as the solution of minimal weighted ℓ_2 norm in the interpolation regime $p > n$:

$$\hat{\boldsymbol{\theta}} = \begin{cases} \arg \min_{\mathbf{w} \in \mathbb{C}^p} \|\mathbf{F}_T \mathbf{w} - \mathbf{y}\|_2^2; & p \leq n \\ \arg \min_{\mathbf{w} \in \mathbb{C}^p} \|\Sigma_T^{-q} \mathbf{w}\|_2^2 \text{ s.t. } \mathbf{F}_T \mathbf{w} = \mathbf{y} & p > n \end{cases}, \quad (4)$$

where $\Sigma_T \in \mathbb{R}^{p \times p}$ is the diagonal matrix as in Def. 2.1 restricted to its first p rows and p columns and $q \geq 0$ controls the rate of growth of the weight. Note that the weight matrix Σ_T^{-q} has no influence on the estimator in the underparameterized regime $p \leq n$. Denoting by \mathbf{A}^\dagger the Moore-Penrose pseudo-inverse of a matrix \mathbf{A} , we can write the solution in both the under- and overparameterized case as

$$\hat{\boldsymbol{\theta}} = \Sigma_T^q (\mathbf{F}_T \Sigma_T^q)^\dagger \mathbf{y}.$$

We will derive sharp non-asymptotic expressions for the risk of the estimator $f_{\hat{\boldsymbol{\theta}}}$ in terms of p, n, D, r , and q . The risk in this setting is defined as

$$\text{risk} = \text{risk}_q = \mathbb{E}_{\boldsymbol{\theta}} \left[\int_{-\pi}^{\pi} |f_{\boldsymbol{\theta}}(x) - f_{\hat{\boldsymbol{\theta}}}(x)|^2 dx \right] = \mathbb{E}_{\boldsymbol{\theta}} \|\boldsymbol{\theta} - \hat{\boldsymbol{\theta}}\|_2^2, \quad (5)$$

where the last equality follows from Parseval's identity.

3 Risk Analysis for Decaying Fourier Series Model

We here derive exact, non-asymptotic expressions for the risk via plain and weighted ℓ_2 regression with Fourier series features, in both the over- and underparameterized regimes. All proofs are deferred to the appendix.

We first focus on the overparameterized regime ($p \geq n$). For ease of exposition, we restrict below to the case where p is an integer multiple of n , but note that the result can be extended to the general case. Moreover, we introduce the notation $t_j = (j+1)^{-1}$, $j \in [D]$ and $\Sigma = \text{diag}([t_0, \dots, t_{D-1}])$. Finally, recall that $c_r = 1 / \sum_{j=0}^{D-1} t_j^{2r}$.

Theorem 1. (Risk in overparameterized regime) Assume $D = \tau n$ and $p = ln$ for $\tau, l \in \mathbb{N}_+ := \{1, 2, \dots\}$, (i.e. $p \geq n$). Let the feature vector $\boldsymbol{\theta}$ be drawn from a distribution with $\mathbb{E}[\boldsymbol{\theta}] = \mathbf{0}$ and $\mathbb{E}[\boldsymbol{\theta}\boldsymbol{\theta}^*] = c_r \Sigma^{2r}$. Then the risks of the regression coefficients $\hat{\boldsymbol{\theta}}$ fitted by plain min-norm estimator ($q = 0$) and weighted min-norm estimator ($q > 0$) (i.e. $\mathbb{E}[\|\boldsymbol{\theta} - \hat{\boldsymbol{\theta}}\|^2]$) are given by

$$\text{risk}_0 = 1 - \frac{n}{p} + \frac{2n}{p} \cdot c_r \sum_{j=p}^{D-1} t_j^{2r}, \quad (6)$$

$$\text{risk}_q = 1 - \underbrace{c_r \sum_{k=0}^{n-1} \frac{\sum_{\nu=0}^{l-1} t_{k+n\nu}^{2q+2r}}{\sum_{\nu=0}^{l-1} t_{k+n\nu}^{2q}}}_{\mathcal{P}_q} + \underbrace{c_r \sum_{k=0}^{n-1} \frac{\left(\sum_{\nu=0}^{l-1} t_{k+n\nu}^{4q}\right) \left(\sum_{\nu=l}^{\tau-1} t_{k+n\nu}^{2r}\right)}{\left(\sum_{\nu=0}^{l-1} t_{k+n\nu}^{2q}\right)^2}}_{\mathcal{Q}_q}. \quad (7)$$

Remark 1.1. While the general risk expressions are difficult to parse, special cases are straightforward: if $p = D$, then $\text{risk}_0 = 1 - \frac{n}{D}$ and, since $\mathcal{Q}_q = 0$ when $l = \tau$, $\text{risk}_q = 1 - \mathcal{P}_q$. Moreover, if $n = p = D$, then $l = \tau = 1$, and hence $\mathcal{P}_q = c_r \sum_{n=0}^{D-1} (t_s^{2q+m} / t_s^{2q}) = 1$ so that $\text{risk}_0 = \text{risk}_q = 0$, as expected.

Proof Sketch For any $u \geq 0$, let $\mathbf{A}_u := \mathbf{F}_T \Sigma_T^u \mathbf{F}_T^*$ and $\mathbf{C}_u := \mathbf{F}_{T^c} \Sigma_{T^c}^u \mathbf{F}_{T^c}^*$. For risk_0 , with $\mathbf{F}_T \mathbf{F}_T^* = p \mathbf{I}_n$ (Lemma 2) and the assumption $\mathbb{E}[\boldsymbol{\theta} \boldsymbol{\theta}^*] = c_r \Sigma^{2r}$, $\text{risk}_0 = 1 - c_r \text{tr}(\mathbf{A}_{2r}) + c_r \text{tr}(\mathbf{C}_{2r})$ (Lemma 1), where the diagonals of \mathbf{A}_{2r} and \mathbf{C}_{2r} can be directly computed. For risk_q , since \mathbf{A}_u and \mathbf{C}_u are circulant matrices (Lemma 2), $\mathbf{A}_u = \mathbf{U}_n \Lambda_{a,u} \mathbf{U}_n^*$ and $\mathbf{C}_u = \mathbf{U}_n \Lambda_{c,u} \mathbf{U}_n^*$, where \mathbf{U}_n is the unitary discrete Fourier matrix with order n . The corresponding eigenvalues $\Lambda_{a,u}$ and $\Lambda_{c,u}$ can also be directly computed. Hence, by Lemma 1, $\text{risk}_q = 1 - c_r \text{tr}(\mathbf{A}_{2q+2r} \mathbf{A}_{2q}^{-1}) + c_r \text{tr}(\mathbf{C}_{2r} \mathbf{A}_{2q}^{-1} \mathbf{A}_{4q} \mathbf{A}_{2q}^{-1})$ has the non-asymptotic closed form as (7).

Using the expressions in Theorem 1, we can quantify how smoothness (as reflected in the rate of decay $r > 0$ in the underlying Fourier series coefficients) can be exploited by setting the weights in the optimization accordingly ($q = r$) to reduce the risk in the overparameterized setting.

Theorem 2. (Rate of weighted min-norm risk) *In the overparameterized setting of Theorem 1, if $q = r > 1/2$ and $p = nl$ with $l \in \mathbb{N}_+$, $l \geq 2$, then the risk of weighted optimization satisfies*

$$\text{risk}_q \leq an^{-2r+1} + bn^{-2r} p^{-2r+1}$$

with

$$a = \frac{2 + d_r n^{-2r}}{(1 + d_r n^{-2r})(1 - (D+1)^{-2r+1})}, \quad b = \frac{d_r}{(1 + d_r n^{-2r})(1 - (D+1)^{-2r+1})},$$

$$d_r = \frac{2^{-2r+1} - (l+1)^{-2r+1}}{2r-1}.$$

Remark 2.1. *For sufficiently large D and n , the constants in the above theorem satisfy $a \leq 2$ and $b \leq 2^{-2r+1}/(2r-1)$ so that then*

$$\text{risk}_q \leq 2n^{-2r+1} + \frac{2}{2r-1} (2n)^{-2r} p^{-2r+1}.$$

In order to fully understand the benefit of overparameterization, we derive the nonasymptotic risk for the estimators in the underparameterized regime ($p \leq n$), where q does not have an influence on the estimators and, hence, on the risk.

Theorem 3. (Risk in underparameterized regime) *Suppose $D = \tau n$ for $\tau \in \mathbb{N}_+$. Suppose $p \leq n$, and assume that the feature vector $\boldsymbol{\theta}$ is drawn from a distribution with $\mathbb{E}[\boldsymbol{\theta}] = \mathbf{0}$ and $\mathbb{E}[\boldsymbol{\theta} \boldsymbol{\theta}^*] = c_r \Sigma^{2r}$. Then the risk ($\mathbb{E}[\|\boldsymbol{\theta} - \hat{\boldsymbol{\theta}}\|^2]$) is given by*

$$\text{risk}_{\text{under}} = c_r \left(\sum_{j=p}^{D-1} t_j^{2r} + \sum_{k=1}^{\tau-1} \sum_{j=0}^{p-1} t_{kn+j}^{2r} \right) \quad (8)$$

Remark 3.1. *When $r = 0$, $\text{risk}_{\text{under}} = \frac{1}{D}(D-p+(\tau-1)p) = 1+p(\frac{1}{n}-\frac{2}{D})$ and the risk increases with p until $p = n$, provided $n < D/2$. From Figure 2 we can see this behavior of the risk curve persist a while, then transition to a U-shape curve, and then transition to a decreasing curve, as we vary r in the range $0 \leq r \leq 1$. For $r \geq 1$, we prove that the risk is monotonically decreasing in p .*

Finally, we show that "the second descent" of the weighted min-norm estimator in the overparameterized regime achieves a lower risk than in the underparameterized regime, provided $q \geq r \geq 1$. In other words, in this case it is definitive that "overparameterization is better than underparameterization".

Theorem 4. (Lowest risk) *In the setting of Theorems 1 and 3, assume that $q \geq r \geq 1$. Then,*

- (a) *In the underparameterized regime ($p \leq n$), the risk is monotonically decreasing in p and the lowest risk in this regime is $\text{risk}_{\text{under}}^* = 2c_r \sum_{j=n}^{D-1} t_j^{2r}$.*
- (b) *The lowest risk in the overparameterized regime ($p > n$) is strictly less than the lowest possible risk in the underparameterized regime.*

Remark 4.1. *While the above theorem holds for any q satisfying $q \geq r \geq 1$, our experiments suggest that $q = r$ is an appropriate choice for any $r \geq 0$, corresponding to the case where the assumed smoothness q employed in the weighted optimization matches the true underlying smoothness r . For a range of choices for r and q , the plots of the theoretical extended risk curves (fixed n , varying p) can be found in the appendix.*

4 Weighted Optimization on Neural Networks and Weight Normalization

Inspired by the fact that weighted ℓ_2 optimization provides better generalization in the Fourier series model, we consider weighted optimization as a strategy more broadly for the ℓ_2 regression problem and general (possibly non-linear) parameterized features, and connect weighted optimization to the Weight Normalization algorithm (Salimans and Kingma, 2016).

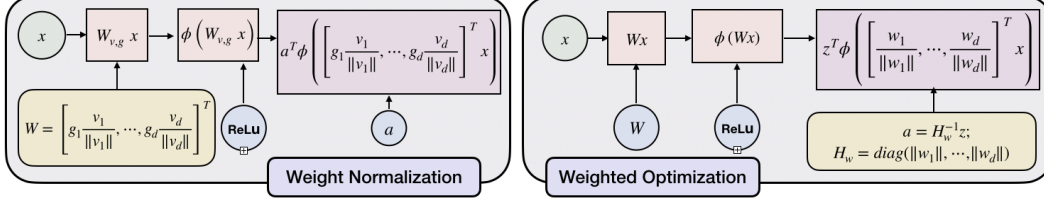


Figure 1: Connection between Weight Normalization and Weighted Optimization.

Weighted optimization for smooth interpolation in overparameterized neural networks For the sake brevity, we will focus on the setting of one-hidden-layer neural networks, where the parameterized function class consists functions of the form $f(\mathbf{x}) = \mathbf{a}^T \phi(\mathbf{W}\mathbf{x})$ with $\Theta := \{\mathbf{W} \in \mathbb{R}^{d \times (m+1)}; \mathbf{a} \in \mathbb{R}^d\}$ the parameters to be optimized (the bias vector is contained in \mathbf{W} and $\mathbf{x} \in \mathbb{R}^{m+1}$ is augmented accordingly), and $\phi(\cdot)$ is a non-linear activation function such as the (Leaky) ReLU activation function. In the ReLU case, we may write $f(\mathbf{x}) = \mathbf{a}^T (\mathbf{D}_{\mathbf{W}\mathbf{x}} \mathbf{W}\mathbf{x})$, where $\mathbf{D}_{\mathbf{W}\mathbf{x}}$ is a diagonal matrix with diagonal terms $(\mathbf{D}_{\mathbf{W}\mathbf{x}})_{k,k} = \mathbf{1}_{(\mathbf{W}\mathbf{x})_k \geq 0} =: \sigma_k$. Note that \mathbf{a}^T generalizes to $\mathbf{A} \in \mathbb{R}^{d_{out} \times d}$ in case of multi-dimensional outputs. The gradient of this function with respect to \mathbf{x} is

$$\nabla f(\mathbf{x}) = \mathbf{W}^T \frac{\partial \phi(\mathbf{W}\mathbf{x})}{\partial \mathbf{W}\mathbf{x}} \mathbf{a} = \mathbf{W}^T \mathbf{D}_{\mathbf{W}\mathbf{x}} \mathbf{a} \quad (9)$$

Assuming that the weight vectors \mathbf{w}_k are close to being orthogonal, we have

$$\|\nabla f(\mathbf{x})\|^2 = \|\mathbf{W}^T \mathbf{D}_{\mathbf{W}\mathbf{x}} \mathbf{a}\|^2 = \left\| \sum_{k=1}^d \sigma_k a_k \mathbf{w}_k \right\|^2 \lesssim \sum_{k=1}^d \sigma_k^2 a_k^2 \|\mathbf{w}_k\|^2 \leq \|\mathbf{H}_w \mathbf{a}\|^2, \quad (10)$$

where $\mathbf{w}_k \in \mathbb{R}^{m+1}$ is the k th row vector of \mathbf{W} and $\mathbf{H}_w = \text{diag}(\|\mathbf{w}_1\|, \|\mathbf{w}_2\|, \dots, \|\mathbf{w}_d\|)$. Note that the inequality \lesssim holds up to an absolute constant in the case of almost orthogonal vectors $\{\mathbf{w}_k\}$ ⁷; the inequality \lesssim holds with constant d for any choice of weight vectors \mathbf{w}_k by equivalence of the ℓ_1 and ℓ_2 norms on \mathbb{R}^d . Thus, we propose an analog of the weighted optimization strategy in (4) (with $q = 1$) by reparameterizing $\mathbf{z} = \mathbf{H}_w \mathbf{a}$ (i.e. $\mathbf{a} = \mathbf{H}_w^{-1} \mathbf{z}$) and considering

$$(\text{weighted optimization}) \quad \min_{\mathbf{z}, \mathbf{W}} \|\mathbf{z}\|^2 \quad \text{s.t.} \quad \mathbf{z}^T \mathbf{H}_w^{-1} \phi(\mathbf{W}\mathbf{x}_i) = y_i, \quad i \in [n]. \quad (11)$$

In contrast to the weighted ℓ_2 -norm optimization we proposed for linear feature interpolation, we now consider the joint optimization over \mathbf{z} and \mathbf{W} . Nevertheless, at a global optimum $(\mathbf{z}^*, \mathbf{W}^*)$, \mathbf{z}^* is the minimizer of the above program with fixed weight \mathbf{W}^* , and by (10) we promote smoothness of the corresponding neural network interpolant. Note that if \mathbf{H}_w were replaced by \mathbf{I} , we would recover the standard min-norm solution.

Since the ReLU activation is scale-invariant, i.e. $\max\{0, cx\} = c \max\{0, x\}, \forall c \geq 0$, and the diagonal elements of \mathbf{H}_w^{-1} are nonnegative, the ℓ_2 loss with weighted optimization is then

$$\mathcal{L}(\mathbf{W}, \mathbf{z}) = \sum_{i=1}^n (\mathbf{z}^T \phi(\mathbf{H}_w^{-1} \mathbf{W}\mathbf{x}_i) - y_i)^2 \quad \text{with} \quad (\mathbf{H}_w^{-1} \mathbf{W})^T = [\frac{\mathbf{w}_1}{\|\mathbf{w}_1\|}, \dots, \frac{\mathbf{w}_d}{\|\mathbf{w}_d\|}] \quad (12)$$

⁷ Initialization with a set of high-dimensional Gaussian vectors is almost orthogonal—see "xavier_normal" and "kaiming_normal" in PyTorch. Moreover, Du et al. (2019) and subsequent works indicate that in a broad class of overparameterized randomly initialized neural networks optimized using gradient descent have the property that the weight vectors must remain close to their initialized values for all iterations.

Weight Normalization (WN) The weighted optimization in (12) is reminiscent of the one-hidden-layer neural network model reparameterized using weight normalization (Salimans and Kingma, 2016) on the first layer, which is as follows:

$$\mathcal{L}(\mathbf{V}_{w,g}, \mathbf{a}) = \sum_{i=1}^n (\mathbf{a}^T \phi(\mathbf{W}_{v,g} \mathbf{x}_i) - y_i)^2 \quad \text{with} \quad \mathbf{W}_{v,g}^T = [g_1 \frac{\mathbf{v}_1}{\|\mathbf{v}_1\|}, \dots, g_d \frac{\mathbf{v}_d}{\|\mathbf{v}_d\|}] \quad (13)$$

Weight Normalization was proposed and previously studied from an optimization perspective, as a way to improve the conditioning of the optimization problem and speed up convergence (Salimans and Kingma, 2016). However, in light of the weighted optimization perspective and its connection to ℓ_2 regularization, we argue that *WN can be interpreted as weighted optimization with $\mathbf{H} = \mathbf{H}_w$ that encourages smooth interpolations*, with secondary trainable parameters $\{g_i\}_{i=1}^d$ to approximate the first order gradient more accurately. This perspective can explain the empirical finding in Van Laarhoven (2017) that explicit ℓ_2 regularization has no regularizing effect when combined with weight normalization.

Details of the connection between weighted optimization and weight normalization are illustrated in Figure 1. From a computational perspective, including \mathbf{H}_w with parameters (i.e. trainable tensors) $\{\mathbf{w}_i\}_{i=1}^d$ in the computational graph⁸, training one-hidden-layer neural networks that contain WN on the first layer with $g_i = 1, i \in [d]$ is equivalent to training the weighted optimization formulation with (stochastic) gradient descent jointly. The intuition from the linear regression case suggests that GD biases towards a small ℓ_2 -norm solution with respect to \mathbf{z} , similar to (11).

Moreover, in our experiments in section 5, by inspection of the training and testing accuracy curves, comparable best test accuracy, and consonant histograms of the norm of the weights, we argue that *weighted optimization performs comparably to weight normalization on large-scale learning problems*. Previous empirical findings also show that only optimizing \mathbf{w} with fixed g in training the last layer of neural networks can improve generalization (Goyal et al., 2017; Xu et al., 2019). Hence, we hypothesize that the scale parameter g in weight normalization is of secondary importance compared to the directional parameters \mathbf{w} , and moreover that weight normalization achieves lower generalization error in part due to an underlying implicit bias towards smoother interpolants.

5 Experiments

Discrete Fourier Models In this experiment, we use Fourier series models $\mathbf{F} \in \mathbb{C}^{n \times D}, D = 1024, n = 64$ with r -decaying multivariate Gaussian coefficients ($r = 0.3, 0.5, 1.0$). $\mathbf{F}_T \in \mathbb{C}^{n \times p}$ is the observation matrix with $p < n$ in underparameterized regime; and $p = ln, l = 1, 2, \dots, \tau$, in the overparameterized regime. The weighted min-norm estimator uses $\Sigma^q, q \geq 0$ to define the weighted ℓ_2 -norm. The theoretical curves are the risks calculated according to Theorem 1 and 3. The empirical mean curves and the 80% confidence intervals (CI) are estimated by 100 runs of independently sampled feature vectors $\boldsymbol{\theta}$.

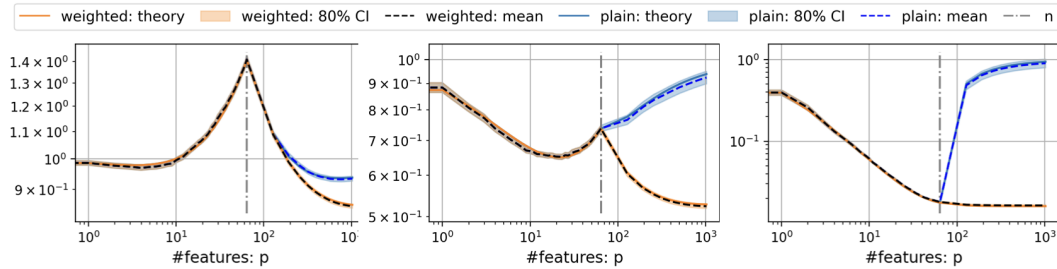


Figure 2: Theoretical and empirical risks ($\|\boldsymbol{\theta} - \hat{\boldsymbol{\theta}}\|^2$) of plain and weighted min-norm estimators in log-log scale. Left to right: $r = q = 0.3, 0.5, 1.0$.

Figure 2 shows that the empirical mean risks match the theoretical risks $\mathbb{E}[\|\boldsymbol{\theta} - \hat{\boldsymbol{\theta}}\|^2]$ of Theorems 1 and 3 very accurately. Figure 2 validates that weighted optimization results in better generalization in

⁸ In the implementation, we multiply the outputs of ReLU (i.e. $\phi(\mathbf{W}\mathbf{x}_i)$) with \mathbf{H}_w^{-1} , where \mathbf{W} is the same set of parameters as in $\phi(\mathbf{W}\mathbf{x}_i)$, and then optimize the parameters with gradients from automatic differentiation.

the overparameterized regime (Theorem 4), and shows non-degenerated double descent curves when $r = q = 0.5$.

Smooth Function Interpolation In this experiment, we implement the discrete Fourier model: $D = 1024, q = 1$ and $f_1(x) : n = 256, p = 512; f_2(x) : n = 64, p = 512$.

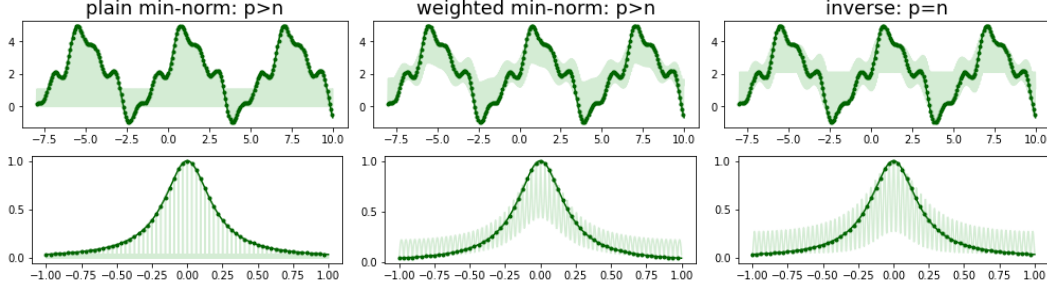


Figure 3: Interpolation of smooth functions. Up: $f_1(x) = 2 \sin(x) + 2 \sin^2(2x) \cos(x) + 0.2 \sin(3x) + 2$. Down: $f_2(x) = 1/(1 + 25x^2)$. Left: interpolation by plain min-norm estimator; Middle: by weighted min-norm estimator; Right: by the inverse with $p = n$.

Figure 3 presents the interpolation (light green) using different estimators with the same set of equispaced samples (dark green). It verifies that the weighted min-norm estimator has better performance, compared to plain min-norm estimator and the inverse with $n = p$, which overlays.

One-Hidden-Layer Neural Networks on MNIST Dataset In this experiment, we compare the following models: plain NN (nmodel), NN with weight normalization (wmodel), NN with weighted optimization (gmodel), NN with batch normalization (bmodel), and bmodel with weighted optimization (bgmodel). We use activation function ReLU, optimizer Adam (Kingma and Ba, 2014) with learning rate $\eta = 0.01$ and step decay $\gamma = 0.1$ per 20 epochs. The number of hidden neurons are $d = 200, 1000, 2000, 5000$.

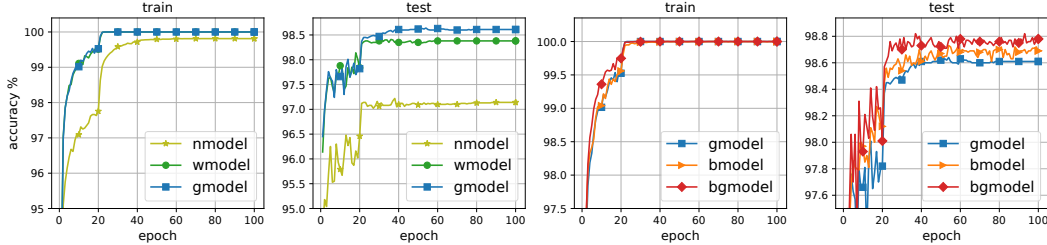


Figure 4: Training and test accuracy of different models on MNIST using overparameterized one-hidden-layer neural networks with #hidden neurons $d = 2000$. Left: comparison of nmodel, gmodel and wmodel; Right: comparison of gmodel, bmodel, and bgmodel.

First, we show how wmodel and gmodel behave similarly with MNIST dataset. Figure 4 (left) indicates that gmodel has almost the same training accuracy curve as wmodel and similar test accuracy curve, and their accuracy are much higher than nmodel. In the case $d = 2000$, gmodel behaves even better than wmodel. With other numbers of hidden neurons (see Table 1), the best accuracy of gmodel and wmodel are close as well. In addition, Figure 5 displays that the corresponding histograms of $\{\|w_i\|^{-1}\}_{i=1}^d$ of gmodel and wmodel at best accuracy have almost the same pattern, while other models include quite different peaks. Second, we argue that weighted optimization is compatible with batch normalization (BN) and combining them can even improve over it. Figure 4 (right) and Table 1 show that combined with BN, bgmodel has the best test accuracy over all models.

Model/d	5000	2000	1000	200
nmodel	97.35	97.22	97.31	97.12
wmodel	98.65	98.42	98.50	98.49
gmodel	98.47	98.64	98.39	98.40
bmodel	98.73	98.73	98.73	98.47
bgmodel	98.86	98.82	98.79	98.62

Table 1: The best test accuracy (%) of different models with different #hidden neurons.

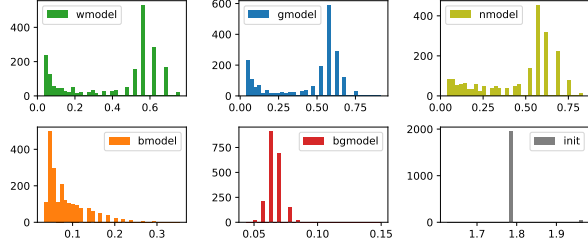


Figure 5: Histogram of H_w^{-1} at best accuracy.

Acknowledgements

R. Ward and Y. Xie were supported in part by AFOSR 2018 MURI Award "Verifiable, Control-Oriented Learning On The Fly". H.H Chou and H. Rauhut were supported in part by the DAAD grant 57417829 "Understanding stochastic gradient descent in deep learning" and by the Excellence Initiative of the German federal and state governments.

References

- Bartlett, P. L., Long, P. M., Lugosi, G., and Tsigler, A. (2020). Benign overfitting in linear regression. *Proceedings of the National Academy of Sciences*.
- Belkin, M., Hsu, D., Ma, S., and Mandal, S. (2019a). Reconciling modern machine-learning practice and the classical bias–variance trade-off. *Proceedings of the National Academy of Sciences*, 116(32):15849–15854.
- Belkin, M., Hsu, D., and Xu, J. (2019b). Two models of double descent for weak features. *arXiv preprint arXiv:1903.07571*.
- Belkin, M., Rakhlin, A., and Tsybakov, A. B. (2018). Does data interpolation contradict statistical optimality? *arXiv preprint arXiv:1806.09471*.
- Canziani, A., Paszke, A., and Culurciello, E. (2016). An analysis of deep neural network models for practical applications. *arXiv preprint arXiv:1605.07678*.
- Du, S. S., Zhai, X., Poczos, B., and Singh, A. (2019). Gradient descent provably optimizes over-parameterized neural networks. In *International Conference on Learning Representations*.
- Geiger, M., Jacot, A., Spigler, S., Gabriel, F., Sagun, L., d’Ascoli, S., Biroli, G., Hongler, C., and Wyart, M. (2020). Scaling description of generalization with number of parameters in deep learning. *Journal of Statistical Mechanics: Theory and Experiment*, 2020(2):023401.
- Ghorbani, B., Mei, S., Misiakiewicz, T., and Montanari, A. (2019). Linearized two-layers neural networks in high dimension. *arXiv preprint arXiv:1904.12191*.
- Goyal, P., Dollár, P., Girshick, R., Noordhuis, P., Wesolowski, L., Kyrola, A., Tulloch, A., Jia, Y., and He, K. (2017). Accurate, large minibatch sgd: Training imagenet in 1 hour. *arXiv preprint arXiv:1706.02677*.
- Hastie, T., Montanari, A., Rosset, S., and Tibshirani, R. J. (2019). Surprises in high-dimensional ridgeless least squares interpolation. *arXiv preprint arXiv:1903.08560*.
- He, K., Zhang, X., Ren, S., and Sun, J. (2015). Delving deep into rectifiers: Surpassing human-level performance on imagenet classification. In *Proceedings of the IEEE international conference on computer vision*, pages 1026–1034.
- Ioffe, S. and Szegedy, C. (2015). Batch Normalization: Accelerating Deep Network Training by Reducing Internal Covariate Shift. *arXiv:1502.03167 [cs]*. arXiv: 1502.03167.
- Kingma, D. P. and Ba, J. (2014). Adam: A method for stochastic optimization. *arXiv preprint arXiv:1412.6980*.

- Liang, T. and Rakhlin, A. (2018). Just interpolate: Kernel" ridgeless" regression can generalize. *arXiv preprint arXiv:1808.00387*.
- Mei, S. and Montanari, A. (2019). The generalization error of random features regression: Precise asymptotics and double descent curve. *arXiv preprint arXiv:1908.05355*.
- Nakkiran, P., Kaplun, G., Bansal, Y., Yang, T., Barak, B., and Sutskever, I. (2019). Deep double descent: Where bigger models and more data hurt. *arXiv preprint arXiv:1912.02292*.
- Rahimi, A. and Recht, B. (2008). Random features for large-scale kernel machines. In *Advances in neural information processing systems*, pages 1177–1184.
- Salimans, T. and Kingma, D. P. (2016). Weight Normalization: A Simple Reparameterization to Accelerate Training of Deep Neural Networks. *arXiv:1602.07868 [cs]*. arXiv: 1602.07868.
- Santurkar, S., Tsipras, D., Ilyas, A., and Madry, A. (2018). How does batch normalization help optimization? In *Advances in Neural Information Processing Systems*, pages 2483–2493.
- Simonyan, K. and Zisserman, A. (2014). Very deep convolutional networks for large-scale image recognition. *arXiv preprint arXiv:1409.1556*.
- Van Laarhoven, T. (2017). L2 regularization versus batch and weight normalization. *arXiv preprint arXiv:1706.05350*.
- Xu, J., Sun, X., Zhang, Z., Zhao, G., and Lin, J. (2019). Understanding and improving layer normalization. In *Advances in Neural Information Processing Systems*, pages 4383–4393.
- Zhang, C., Bengio, S., Hardt, M., Recht, B., and Vinyals, O. (2016). Understanding deep learning requires rethinking generalization. *arXiv preprint arXiv:1611.03530*.

Supplementary Material

Supplementary material for the paper: "Weighted Optimization: better generalization through smooth interpolation". This supplementary material is organized as follows:

- Appendix A: Proof of Theorem 1
- Appendix B: Proof of Theorem 2
- Appendix C: Proof of Theorem 3
- Appendix D: Proof of Theorem 4
- Appendix E: Proof of Lemmas
- Appendix F: Visualization of Theoretical Risks

A Proof of Theorem 1

The proof is based on the following lemmas. Below, the matrix $\mathbf{F}_{T^c} \in \mathbb{C}^{n \times (D-p)}$ is the submatrix of \mathbf{F} corresponding to the columns in $T^c = \{0, 1, \dots, D-1\} \setminus T$.

Lemma 1. (Risks of weighted and plain min-norm estimators in overparameterized regime) Assume $p \geq n$ and let the feature vector $\boldsymbol{\theta} \in \mathbb{C}^D$ be drawn from a distribution with $\mathbb{E}[\boldsymbol{\theta}] = \mathbf{0}$ and $\mathbb{E}[\boldsymbol{\theta}\boldsymbol{\theta}^*] = \mathbf{K}$, where \mathbf{K} is a diagonal matrix. Then the risk of the weighted min-norm estimator with $q \geq 0$ is

$$\text{risk}_q = \mathbb{E}[\|\boldsymbol{\theta} - \hat{\boldsymbol{\theta}}\|^2] = \text{tr}(\mathbf{K}) - \mathcal{P}_q + \mathcal{Q}_q,$$

where

$$\begin{aligned} \mathcal{Q}_q &= \text{tr} \left(\mathbf{F}_T \Sigma_T^{4q} \mathbf{F}_T^* (\mathbf{F}_T \Sigma_T^{2q} \mathbf{F}_T^*)^{-1} \mathbf{F}_{T^c} \mathbf{K}_{T^c} \mathbf{F}_{T^c}^* (\mathbf{F}_T \Sigma_T^{2q} \mathbf{F}_T^*)^{-1} \right), \\ \mathcal{P}_q &= \text{tr} \left(\mathbf{F}_T \Sigma_T^{2q} \mathbf{K}_T \mathbf{F}_T^* (\mathbf{F}_T \Sigma_T^{2q} \mathbf{F}_T^*)^{-1} \right). \end{aligned}$$

Note that the risk of the plain min-norm solution corresponds to $q = 0$.

Lemma 2. (Properties of \mathbf{F} st) Assume that $D = \tau n$ and $p = nl$ for $\tau, l \in \mathbb{N}_+$. Then, $\mathbf{F}_T \mathbf{F}_T^* = p \mathbf{I}_n$. Moreover, for $u \in \mathbb{N}_+$, define $\mathbf{A}_u := \mathbf{F}_T \Sigma_T^u \mathbf{F}_T^*$ and $\mathbf{C}_u := \mathbf{F}_{T^c} \Sigma_{T^c}^u \mathbf{F}_{T^c}^*$, where Σ is a diagonal matrix (for example, the diagonal matrix in (3)). Then, \mathbf{A}_u and \mathbf{C}_u are circulant matrices.

The proofs of Lemma 1 and 2 can be found in Appendix E.

A.1 Proof of the risk of the plain min-norm estimator in Theorem 1

Proof. Lemma 1, with $\mathbf{K} = c_r \Sigma^{2r}$ gives

$$\text{risk}_0 = 1 - c_r \text{tr} \left(\mathbf{F}_T \Sigma_T^{2r} \mathbf{F}_T^* (\mathbf{F}_T \mathbf{F}_T^*)^{-1} \right) + c_r \text{tr} \left(\mathbf{F}_{T^c} \mathbf{K}_{T^c} \mathbf{F}_{T^c}^* (\mathbf{F}_T \mathbf{F}_T^*)^{-1} \right). \quad (14)$$

By Lemma 2, we have $\mathbf{F}_T \mathbf{F}_T^* = p \mathbf{I}_p$, so that

$$\mathcal{P}_1 = \frac{1}{p} \text{tr} (c_r \mathbf{F}_T \Sigma_T^{2r} \mathbf{F}_T^*) = \frac{c_r}{p} \text{tr} (\mathbf{A}_{2r}) \quad \text{and} \quad \mathcal{Q}_1 = \frac{1}{p} \text{tr} (c_r \mathbf{F}_{T^c} \Sigma_{T^c}^{2r} \mathbf{F}_{T^c}^*) = \frac{c_r}{p} \text{tr} (\mathbf{C}_{2r}). \quad (15)$$

The diagonal entries of \mathbf{A}_{2r} and \mathbf{C}_{2r} are given by

$$\mathbf{A}_{2r}^{(i,i)} = \sum_{j=0}^{p-1} t_j^{2r} \exp(0) = \sum_{j=0}^{p-1} t_j^{2r} \quad \text{and} \quad \mathbf{C}_{2r}^{(i,i)} = \sum_{j=0}^{D-1} t_j^{2r} \exp(0) = \sum_{j=p}^{D-1} t_j^{2r}, \quad i \in [n]. \quad (16)$$

It follows that

$$\mathcal{P}_0 = \frac{c_r}{p} \text{tr} (\mathbf{A}_{2r}) = \frac{nc_r}{p} \sum_{j=0}^{p-1} t_j^{2r} \quad \text{and} \quad \mathcal{Q}_0 = \frac{c_r}{p} \text{tr} (\mathbf{C}_{2r}) = \frac{nc_r}{p} \sum_{j=p}^{D-1} t_j^{2r}$$

so that the risk is given by

$$\text{risk}_0 = \mathbb{E}[\|\boldsymbol{\theta} - \hat{\boldsymbol{\theta}}\|^2] = 1 - \frac{nc_r}{p} \left(\frac{1}{c_r} - 2 \sum_{j=p}^{D-1} t_j^{2r} \right) = 1 - \frac{n}{p} + \frac{2n}{p} \cdot \frac{\sum_{j=p}^{D-1} t_j^{2r}}{\sum_{j=0}^{D-1} t_j^{2r}}. \quad \square$$

A.2 Proof of the risk of the weighted min-norm estimator in Theorem 1

Proof. Since A_u and C_u are circulant matrices we can write $A_u = U_n \Lambda_{a,u} U_n^*$ and $C_u = U_n \Lambda_{c,u} U_n^*$, where U_n is the unitary discrete Fourier matrix of size n , and $\Lambda_{a,u}$ and $\Lambda_{c,u}$ are the diagonal matrices with eigenvalues of A_u and C_u , respectively, on the diagonal. The eigenvalues can be calculated by taking discrete Fourier transform of the first column of A_u or C_u .

Let F_n be the n th order discrete Fourier matrix, i.e., $(F_n)_{s,j} = \omega_n^{sj}$, then for any $s \in [n]$, the s th diagonal element (eigenvalue) of $\Lambda_{a,u}$ or $\Lambda_{c,u}$ is

$$\begin{aligned}\lambda_{a,u}^{(s)} &= F_n[s, :] A_u[:, 0] = \sum_{j=0}^{n-1} \omega_n^{sj} \left(\sum_{\nu=0}^{l-1} \sum_{k=0}^{n-1} t_{k+n\nu}^u \omega_n^{-jk} \right) = \sum_{k=0}^{n-1} \left(\sum_{\nu=0}^{l-1} t_{k+n\nu}^u \right) \left(\sum_{j=0}^{n-1} \omega_n^{(s-k)j} \right) \\ \lambda_{c,u}^{(s)} &= F_n[s, :] C_u[:, 0] = \sum_{j=0}^{n-1} \omega_n^{sj} \left(\sum_{\nu=l}^{\tau-1} \sum_{k=0}^{n-1} t_{k+n\nu}^u \omega_n^{-jk} \right) = \sum_{k=0}^{n-1} \left(\sum_{\nu=l}^{\tau-1} t_{k+n\nu}^u \right) \left(\sum_{j=0}^{n-1} \omega_n^{(s-k)j} \right)\end{aligned}$$

For $s, k \in [n]$ we define

$$e_{s,k}^{(n)} := \sum_{j=0}^{n-1} \omega_n^{(s-k)j} = \begin{cases} n, & \text{if } k = s, \\ 0, & \text{otherwise.} \end{cases} \quad (17)$$

If the random Fourier series has r -decaying coefficients, i.e., $K = c_r \Sigma^{2r}$ ($r \geq 0$), then by Lemma 1,

$$\begin{aligned}\mathcal{P}_q &= c_r \text{tr} \left(F_T \Sigma_T^{2q+2r} F_T^* (F_T \Sigma_T^{2q} F_T^*)^{-1} \right) = c_r \text{tr} \left(U_n \Lambda_{a,2q+2r} U_n^* U_n \Lambda_{a,2q}^{-1} U_n^* \right) \\ &= c_r \text{tr} \left(\Lambda_{a,2q+2r} \Lambda_{a,2q}^{-1} \right) = c_r \sum_{s=0}^{n-1} \frac{\sum_{k=0}^{n-1} \left(\sum_{\nu=0}^{l-1} t_{k+n\nu}^{2q+2r} \right) e_{s,k}^{(n)}}{\sum_{k=0}^{n-1} \left(\sum_{\nu=0}^{l-1} t_{k+n\nu}^{2q} \right) e_{s,k}^{(n)}} \\ &= \frac{1}{\sum_{j=0}^{D-1} t_j^{2r}} \sum_{k=0}^{n-1} \frac{\sum_{\nu=0}^{l-1} t_{k+n\nu}^{2q+2r}}{\sum_{\nu=0}^{l-1} t_{k+n\nu}^{2q}},\end{aligned}$$

and

$$\begin{aligned}\mathcal{Q}_q &= c_r \text{tr} \left(F_{T^c} \Sigma_{T^c}^{2r} F_{T^c}^* (F_T \Sigma_T^{2q} F_T^*)^{-1} F_T \Sigma_T^{4q} F_T^* (F_T \Sigma_T^{2q} F_T^*)^{-1} \right) \\ &= c_r \text{tr} \left(U_n \Lambda_{c,2r} U_n^* U_n \Lambda_{a,2q}^{-1} U_n^* U_n \Lambda_{a,4q} U_n^* U_n \Lambda_{a,2q}^{-1} U_n^* \right) = c_r \text{tr} \left(\Lambda_{c,2r} \Lambda_{a,2q}^{-1} \Lambda_{a,4q} \Lambda_{a,2q}^{-1} \right) \\ &= c_r \sum_{s=0}^{n-1} \frac{\left(\sum_{k=0}^{n-1} \left(\sum_{\nu=0}^{l-1} t_{k+n\nu}^{4q} \right) e_{s,k}^{(n)} \right) \left(\sum_{k=0}^{n-1} \left(\sum_{\nu=l}^{\tau-1} t_{k+n\nu}^{2r} \right) e_{s,k}^{(n)} \right)}{\left(\sum_{k=0}^{n-1} \left(\sum_{\nu=0}^{l-1} t_{k+n\nu}^{2q} \right) e_{s,k}^{(n)} \right)^2} \\ &= c_r \sum_{k=0}^{n-1} \frac{\left(\sum_{\nu=0}^{l-1} t_{k+n\nu}^{4q} \right) \left(\sum_{\nu=l}^{\tau-1} t_{k+n\nu}^{2r} \right)}{\left(\sum_{\nu=0}^{l-1} t_{k+n\nu}^{2q} \right)^2}.\end{aligned}$$

Therefore, the risk satisfies

$$\begin{aligned}\text{risk}_q &= 1 - \mathcal{P}_q + \mathcal{Q}_q \\ &= 1 - c_r \sum_{k=0}^{n-1} \frac{\sum_{\nu=0}^{l-1} t_{k+n\nu}^{2q+2r}}{\sum_{\nu=0}^{l-1} t_{k+n\nu}^{2q}} + c_r \sum_{k=0}^{n-1} \frac{\left(\sum_{\nu=0}^{l-1} t_{k+n\nu}^{4q} \right) \left(\sum_{\nu=l}^{\tau-1} t_{k+n\nu}^{2r} \right)}{\left(\sum_{\nu=0}^{l-1} t_{k+n\nu}^{2q} \right)^2}.\end{aligned} \quad \square$$

B Proof of Theorem 2

We start with a lemma on the normalizing constant c_r .

Lemma 3. For $r > 1/2$, the constant $c_r = (\sum_{j=0}^{D-1} t_j^{2r})^{-1}$ satisfies

$$\frac{2r-1}{2r-D^{-2r+1}} \leq c_r \leq \min \left\{ \frac{2r-1}{1-(D+1)^{-2r+1}}, \frac{2r-1}{2r-1+2^{-2r+1}-(D+1)^{-2r+1}} \right\}.$$

Proof. By comparison of the sum to an integral we have

$$\sum_{j=0}^{D-1} t_j^{2r} = \sum_{j=1}^D \frac{1}{j^{2r}} \geq \int_1^{D+1} \frac{1}{x^{2r}} dx = \frac{1}{2r-1} (1 - (D+1)^{-2r+1}).$$

Alternatively,

$$\begin{aligned} \sum_{j=0}^{D-1} t_j^{2r} &= 1 + \sum_{j=2}^D \frac{1}{j^{2r}} \geq 1 + \int_2^{D+1} \frac{1}{x^{2r}} dx = 1 + \frac{1}{2r-1} (2^{-2r+1} - (D+1)^{-2r+1}) \\ &= \frac{1}{2r-1} (2r-1 + 2^{-2r+1} - (D+1)^{-2r+1}). \end{aligned}$$

Similarly, we obtain

$$\begin{aligned} \sum_{j=0}^{D-1} t_j^{2r} &= 1 + \sum_{j=2}^D \frac{1}{k^{2r}} \leq 1 + \int_1^D \frac{1}{x^{2r}} dx = 1 + \frac{1}{2r-1} (1 - D^{-2r+1}) \\ &= \frac{1}{2r-1} (2r - D^{-2r+1}). \end{aligned}$$

This concludes the proof by taking inverses. \square

Proof of Theorem 2. For $k \in [n]$ and $\alpha \in \mathbb{R}$, we define

$$A(k, \alpha) := \sum_{\nu=0}^{l-1} t_{k+n\nu}^\alpha \quad \text{and} \quad B(k, \alpha) = \sum_{\nu=1}^{l-1} t_{k+n\nu}^\alpha = A(k, \alpha) - \frac{1}{(1+k)^\alpha},$$

where we understand that $B(k, \alpha) = 0$ if $l = 1$. By Theorem 1 we can write

$$\begin{aligned} 1 - \mathcal{P}_q &= c_r \left(c_r^{-1} - \sum_{k=0}^{n-1} \frac{A(k, 2q+2r)}{A(k, 2q)} \right) \\ &= c_r \left(\sum_{k=0}^{n-1} \underbrace{\left(\frac{1}{(1+k)^{2r}} - \frac{A(k, 2q+2r)}{A(k, 2q)} \right)}_{=: \gamma_k} + \sum_{k=n}^{D-1} \frac{1}{(1+k)^{2r}} \right). \end{aligned}$$

We have

$$\begin{aligned} \gamma_{k-1} &= \frac{1}{k^{2r}} - \frac{\frac{1}{k^{2q+2r}} + B(k-1, 2q+2r)}{\frac{1}{k^{2q}} + B(k-1, 2q)} = \frac{1}{k^{2r}} - \frac{1 + k^{2q+2r} B(k-1, 2q+2r)}{k^{2r} + k^{2r+2q} B(k-1, 2q)} \\ &= \frac{1 + k^{2q} B(k-1, 2q) - 1 - k^{2q+2r} B(k-1, 2q+2r)}{k^{2r} (1 + k^{2q} B(k-1, 2q))} \\ &= \frac{k^{2q} B(k-1, 2q) - k^{2q+2r} B(k-1, 2q+2r)}{k^{2r} (1 + k^{2q} B(k-1, 2q))}. \end{aligned}$$

Furthermore, if $l = 1$ (i.e., $p = n$) then the numerator in the last expression vanishes and for $l > 1$ it satisfies

$$\begin{aligned} k^{2q} B(k-1, 2q) - k^{2q+2r} B(k-1, 2q+2r) &= \sum_{\nu=1}^{l-1} \left(\frac{k}{k+n\nu} \right)^{2q} - \sum_{\nu=1}^{l-1} \left(\frac{k}{k+n\nu} \right)^{2q+2r} \\ &= \sum_{\nu=1}^{l-1} \left(\frac{k}{k+n\nu} \right)^{2q} \left(1 - \left(\frac{k}{k+n\nu} \right)^{2r} \right). \end{aligned}$$

Altogether, we have that $1 - \mathcal{P}_q = c_r \sum_{k=n+1}^D k^{-2r}$ if $l = 1$ and for $l > 1$ it holds

$$1 - \mathcal{P}_q = c_r \sum_{\nu=1}^{l-1} \sum_{k=1}^n \frac{k^{2q-2r}}{1 + k^{2q} B(k-1, 2q)} \frac{1}{(k + n\nu)^{2q}} \left(1 - \left(\frac{k}{k + n\nu} \right)^{2r} \right) + c_r \sum_{k=n+1}^D \frac{1}{k^{2r}}. \quad (18)$$

For $r \neq 1/2$, the last sum above satisfies

$$\sum_{k=n+1}^D \frac{1}{k^{2r}} \leq \int_n^D x^{-2r} dx = \frac{1}{2r-1} (n^{-2r+1} - D^{-2r+1}),$$

so that $\sum_{k=n+1}^D \frac{1}{k^{2r}} \leq (2r-1)^{-1} n^{-2r+1}$ if $r > 1/2$. (A similar upper bound can be shown as well.) For the following we generally assume that $r, q > 1/2$. Observe that

$$\begin{aligned} B(k-1, 2q) &= \sum_{\nu=1}^{l-1} \left(\frac{1}{k + n\nu} \right)^{2q} \geq \int_1^l \frac{1}{(k + nx)^{2q}} dx = \frac{1}{n} \int_n^{nl} \frac{1}{(k + z)^{2q}} dz \\ &= \frac{1}{n(2q-1)} ((k+n)^{-2q+1} - (k+p)^{-2q+1}), \end{aligned}$$

where we also used that $p = ln$. Since the last expression is decreasing with $k \in \{1, \dots, n\}$, we obtain the lower bound

$$\begin{aligned} B(k-1, 2q) &\geq \frac{1}{n(2q-1)} ((2n)^{-2q+1} - ((l+1)n)^{-2q+1}) = \frac{d_q}{n^{2q}}, \\ \text{where } d_q &:= \frac{2^{-2q+1} - (l+1)^{-2q+1}}{2q-1}. \end{aligned}$$

Hence, we have

$$\begin{aligned} 1 - \mathcal{P}_q &\leq \frac{c_r}{1 + d_q n^{-2q}} \sum_{\nu=1}^{l-1} \sum_{k=1}^n \frac{k^{2q-2r}}{(k + n\nu)^{2q}} \left(1 - \left(\frac{k}{k + n\nu} \right)^{2r} \right) + \frac{c_r}{2r-1} n^{-2r+1} \\ &\leq \frac{c_r}{1 + d_q n^{-2q}} \sum_{\nu=1}^{l-1} \sum_{k=1}^n \frac{k^{2q-2r}}{(k + n\nu)^{2q}} + \frac{c_r}{2r-1} n^{-2r+1}. \end{aligned}$$

If $q = r$ then the double sum above can be estimated as

$$\sum_{\nu=1}^{l-1} \sum_{k=1}^n \frac{1}{(k + n\nu)^{2q}} = \sum_{j=n}^p \frac{1}{j^{2q}} \leq \int_n^p \frac{1}{x^{2q}} dx = \frac{1}{2q-1} (n^{-2q+1} - p^{-2q+1}).$$

Altogether, for $r = q > 1/2$ and $p = ln$ for $l \geq 2$,

$$\begin{aligned} 1 - \mathcal{P}_q &\leq \frac{c_r}{2r-1} \left(\frac{n^{-2r+1} - p^{-2r+1}}{1 + d_r n^{-2r}} + n^{-2r+1} \right) \\ &\leq \frac{1}{1 - (D+1)^{-2r+1}} \left(\frac{n^{-2r+1} - p^{-2r+1}}{1 + d_r n^{-2r}} + n^{-2r+1} \right), \end{aligned}$$

where we have used Lemma 3 in the last step.

It remains to bound \mathcal{Q}_q from above. Towards this goal, we observe the simple inequality

$$\sum_{\nu=0}^{l-1} t_{k+n\nu}^{4q} \leq \left(\sum_{\nu=0}^{l-1} t_{k+n\nu}^{2q} \right)^2.$$

Thus, we have the immediate bound

$$\begin{aligned} \mathcal{Q}_q &\leq c_r \sum_{k=0}^{n-1} \sum_{\nu=l}^{\tau-1} t_{k+n\nu}^{2r} = c_r \sum_{k=p+1}^D \frac{1}{k^{2r}} \leq c_r \int_p^D x^{-2r} dx = \frac{c_r}{2r-1} (p^{-2r+1} - D^{-2r+1}) \\ &\leq \frac{p^{-2r+1}}{1 - (D+1)^{-2r+1}}. \end{aligned}$$

Altogether, for $r = q > 1/2$ and $p = ln$ with $l \geq 2$,

$$\begin{aligned} \text{risk}_q &= 1 - \mathcal{P}_q + \mathcal{Q}_q \\ &\leq \frac{1}{1 - (D+1)^{-2r+1}} \left(\left(\frac{1}{1 + d_r n^{-2r}} + 1 \right) n^{-2r+1} + \left(1 - \frac{1}{1 + d_r n^{-2r}} \right) p^{-2r+1} \right) \\ &= \frac{1}{1 - (D+1)^{-2r+1}} \left(\frac{2 + d_r n^{-2r}}{1 + d_r n^{-2r}} n^{-2r+1} + \frac{d_r}{1 + d_r n^{-2r}} n^{-2r} p^{-2r+1} \right). \end{aligned} \quad (19)$$

The previous expression can be bounded by Cn^{-2r+1} for a suitable constant C .

If $l = 1$ so that $p = n$ then the above derivations give

$$\text{risk}_q = 1 - \mathcal{P}_q + \mathcal{Q}_q \leq \frac{1}{1 - (D+1)^{-2r+1}} (n^{-2r+1} + p^{-2r+1}) = \frac{2}{1 - (D+1)^{-2r+1}} n^{-2r+1},$$

which gives the statement of the theorem also in this case. \square

Note that for large n, p, D the bound (19) roughly reads

$$\text{risk}_q \lesssim 2n^{-2r+1} + \frac{2}{2r-1} (2n)^{-2r} p^{-2r+1},$$

taking into account that $d_r \leq 2^{-2r+1}/(2r-1)$.

C Proof of Theorem 3

The proof of Theorem 3 is based on the following lemma whose proof is contained in Appendix E.

Lemma 4. (Risks of weighted and plain min-norm estimator in the underparameterized regime) *Let the feature vector θ be sampled from a distribution with $\mathbb{E}[\theta] = \mathbf{0}$ and $\mathbb{E}[\theta\theta^*] = \mathbf{K}$. In the underparameterized regime ($p \leq n$), the regression coefficients $\hat{\theta}$ are fitted by weighted least squares with Σ^q as the re-parameterization matrix, then for any $q \geq 0$, $\hat{\theta}_T = (\mathbf{F}_T^* \mathbf{F}_T)^{-1} \mathbf{F}_T^* \mathbf{y}$, $\hat{\theta}_{T^c} = \mathbf{0}$, where $\mathbf{y} = \mathbf{F}_T \theta_T + \mathbf{F}_{T^c} \theta_{T^c}$. The risk is given by*

$$\text{risk}_{\text{under}} = \mathbb{E}[\|\theta - \hat{\theta}\|^2] = \text{tr}(\mathbf{K}_{T^c}) + \text{tr}(\mathbf{F}_T (\mathbf{F}_T^* \mathbf{F}_T)^{-2} \mathbf{F}_T^* \mathbf{F}_{T^c} \mathbf{K}_{T^c} \mathbf{F}_{T^c}^*).$$

Proof of Theorem 3. Denoting $\omega_n = \exp(-\frac{2\pi i}{n})$ we have, for $k_1, k_2 \in [p]$ with $p < n$,

$$(\mathbf{F}_T^* \mathbf{F}_T)_{k_1, k_2} = \sum_{j=0}^{n-1} \exp\left(-\frac{2\pi i}{n} k_1 \cdot j\right) \exp\left(\frac{2\pi i}{n} k_2 \cdot j\right) = \sum_{j=0}^{n-1} \omega_n^{(k_1 - k_2) \cdot j} = \begin{cases} n, & \text{if } k_1 = k_2, \\ 0, & \text{otherwise.} \end{cases}$$

Moreover, for $0 \leq k_1, k_2 \leq D - p - 1$, we have

$$\begin{aligned} (\mathbf{F}_{T^c}^* \mathbf{F}_{T^c})_{k_1, k_2} &= \sum_{j=0}^{n-1} \exp\left(-\frac{2\pi i}{n} (k_1 + p) \cdot j\right) \exp\left(\frac{2\pi i}{n} (k_2 + p) \cdot j\right) = \sum_{j=0}^{n-1} \omega_n^{(k_1 - k_2) \cdot j} \\ &= \begin{cases} n, & \text{if } \exists \gamma \in \mathbb{N}, \text{ s.t. } k_1 - k_2 = \gamma n, \\ 0, & \text{otherwise.} \end{cases} \end{aligned}$$

Since $D = \tau n$ and $0 < p < n$ it holds $v = D - p - n \cdot \lfloor \frac{D-p}{n} \rfloor = n - p$ and $p = n - v$. Introducing the matrices $\mathbf{M}_{n \times v} = \begin{bmatrix} \mathbf{I}_{v \times v} \\ \mathbf{O}_{p \times v} \end{bmatrix}$, $\mathbf{N}_{v \times n} = [\mathbf{I}_{v \times v} \quad \mathbf{O}_{v \times p}]$, $\mathbf{I}_{n, v} = \mathbf{M}_{n \times v} \mathbf{N}_{v \times n} = \begin{bmatrix} \mathbf{I}_{v \times v} & \mathbf{O}_{v \times p} \\ \mathbf{O}_{p \times v} & \mathbf{O}_{p \times p} \end{bmatrix}$, we can write

$$\begin{aligned} (\mathbf{F}_{T^c}^* \mathbf{F}_{T^c})^2 &= n^2 \begin{bmatrix} \mathbf{I}_n & \cdots & \mathbf{I}_n & \mathbf{M}_{n \times v} \\ \vdots & \ddots & \vdots & \vdots \\ \mathbf{I}_n & \cdots & \mathbf{I}_n & \mathbf{M}_{n \times v} \\ \mathbf{N}_{v \times n} & \cdots & \mathbf{N}_{v \times n} & \mathbf{I}_{v \times v} \end{bmatrix}^2 \\ &= n^2 \begin{bmatrix} (\tau-1)\mathbf{I}_n + \mathbf{I}_{n, v} & \cdots & (\tau-1)\mathbf{I}_n + \mathbf{I}_{n, v} & \tau\mathbf{M}_{n \times v} \\ \vdots & \ddots & \vdots & \vdots \\ (\tau-1)\mathbf{I}_n + \mathbf{I}_{n, v} & \cdots & (\tau-1)\mathbf{I}_n + \mathbf{I}_{n, v} & \tau\mathbf{M}_{n \times v} \\ \tau\mathbf{N}_{v \times n} & \cdots & \tau\mathbf{N}_{v \times n} & \tau\mathbf{I}_{v \times v} \end{bmatrix} \triangleq n^2 \mathbf{L}. \end{aligned}$$

Since $\mathbf{F}_T \mathbf{F}_T^* + \mathbf{F}_{T^c} \mathbf{F}_{T^c}^* = D \mathbf{I}_n$ the risk is given as

$$\begin{aligned}
\mathbb{E}[\|\boldsymbol{\theta} - \hat{\boldsymbol{\theta}}\|^2] &= c_r \text{tr}(\Sigma_{T^c}^{2r}) + \frac{c_r}{n^2} \text{tr}((D \mathbf{I}_n - \mathbf{F}_{T^c} \mathbf{F}_{T^c}^*) \mathbf{F}_{T^c} \Sigma_{T^c}^{2r} \mathbf{F}_{T^c}^*) \\
&= c_r \text{tr}(\Sigma_{T^c}^{2r}) + \frac{c_r}{n^2} \text{tr}((D \mathbf{F}_{T^c}^* \mathbf{F}_{T^c} - (\mathbf{F}_{T^c}^* \mathbf{F}_{T^c})^2) \Sigma_{T^c}^{2r}) \\
&= c_r(1 + \tau) \text{tr}(\Sigma_{T^c}^{2r}) - c_r \text{tr}(\mathbf{L} \Sigma_{T^c}^{2r}) \\
&= c_r(1 + \tau) \text{tr}(\Sigma_{T^c}^{2r}) - c_r \tau \text{tr}(\Sigma_{T^c}^{2r}) + c_r \sum_{k=1}^{\tau-1} \sum_{j=0}^{p-1} t_{kn+j}^{2r} \\
&= c_r \sum_{j=p}^{D-1} t_j^{2r} + c_r \sum_{k=1}^{\tau-1} \sum_{j=0}^{p-1} t_{kn+j}^{2r} = \frac{\sum_{j=p}^{D-1} t_j^{2r} + \sum_{k=1}^{\tau-1} \sum_{j=0}^{p-1} t_{kn+j}^{2r}}{\sum_{j=0}^{D-1} t_j^{2r}}. \quad \square
\end{aligned}$$

D Proof of Theorem 4

Proof of Theorem 4. (a) We show that, for fixed n and $r \geq 1$, the risk in the underparameterized setting is monotonically decreasing in p . To this end we set $f(p) = \sum_{j=p}^{D-1} t_j^{2r} + \sum_{k=1}^{\tau-1} \sum_{j=0}^{p-1} t_{kn+j}^{2r}$, where $t_j = (j+1)^{-1}$. Let $\Delta_r(p) = f(p+1) - f(p)$, for $0 \leq p \leq n-1$, be the increment. Then $\Delta(p) = -t_p^{2r} + \sum_{k=1}^{\tau-1} t_{kn+p}^{2r}$. The goal is to show $\Delta \leq 0$. By monotonicity of the function $g(x) = (nx + p + 1)^{-2r}$, we have

$$\sum_{k=1}^{\tau-1} t_{kn+p}^{2r} \leq \int_0^{\tau-1} (nx + p + 1)^{-2r} dx = \frac{1}{n(1-2r)} [(n(\tau-1) + p + 1)^{1-2r} - (p+1)^{1-2r}].$$

It follows that

$$\Delta(p) \leq -(p+1)^{-2r} + \frac{1}{n(1-2r)} [(n(\tau-1) + p + 1)^{1-2r} - (p+1)^{1-2r}] =: \Delta^+(p).$$

Hence it suffices to show that $\Delta^+(p) \leq 0$, for $0 \leq p \leq n-1$. Its derivative with respect to p is given by

$$\begin{aligned}
\Delta^{+'}(p) &= 2r(p+1)^{-2r-1} + \frac{1}{n} [(n(\tau-1) + p + 1)^{-2r} - (p+1)^{-2r}] \\
&= (p+1)^{-2r} \underbrace{\left(2r(p+1)^{-1} - \frac{1}{n} \right)}_{\alpha(p)} + \frac{1}{n} (n(\tau-1) + p + 1)^{-2r}.
\end{aligned}$$

We conclude that, for $2r \geq 1$ (implied by $r \geq 1$), $\Delta^{+'} \geq 0$ since $\alpha(p) \geq \frac{2r-1}{n} \geq 0$ as $p \leq n-1$. Because Δ^+ is increasing, it suffices to check if the end point, $\Delta^+(n-1)$, is non-positive in order to ensure $\Delta^+ \leq 0$. Indeed,

$$\begin{aligned}
\Delta^+(n-1) &= -n^{-2r} + \frac{1}{n(1-2r)} [(n\tau)^{1-2r} - n^{1-2r}] = -n^{-2r} + \frac{n^{-2r}}{2r-1} [1 - \tau^{1-2r}] \\
&= -n^{-2r} \underbrace{\left(1 - \frac{1}{2r-1} \right)}_{\beta(r)} - \frac{n^{-2r} \tau^{1-2r}}{2r-1}.
\end{aligned}$$

For $r \geq 1$, $\Delta^+(n-1) \leq 0$ since $\beta(r) \geq 0$. Hence, $r \geq 1$ is a sufficient condition for $\Delta \leq 0$. In this case, the lowest risk is at $p = n$ and takes the value

$$\text{risk}_{\text{under}}^* = 2c_r \sum_{j=n}^{D-1} t_j^{2r}$$

(b) Next we consider two cases in the overparameterized regime: $p = n$ and $p = D$.

When $p = n$ (i.e., $l = 1$), the risk can be written as

$$\text{risk}_q(p = n) = 1 - c_r \sum_{k=0}^{n-1} t_k^{2r} + c_r \sum_{k=0}^{n-1} \sum_{\nu=l}^{\tau-1} t_{k+n\nu}^{2r} = 1 - c_r \sum_{k=0}^{n-1} \underbrace{\left(t_k^{2r} - \sum_{\nu=1}^{\tau-1} t_{k+n\nu}^{2r} \right)}_{=:b_k}.$$

When $p = D$ (i.e., $l = \tau$), we have $\mathcal{Q}_q = 0$ so that

$$\text{risk}_q(p = D) = 1 - c_r \sum_{k=0}^{n-1} \frac{\sum_{\nu=0}^{l-1} t_{k+n\nu}^{2q+2r}}{\sum_{\nu=0}^{l-1} t_{k+n\nu}^{2q}} = 1 - c_r \sum_{k=0}^{n-1} \underbrace{\frac{\sum_{\nu=0}^{\tau-1} t_k^{2q+2r}}{t_k^{2q} + \sum_{\nu=1}^{\tau-1} t_{k+n\nu}^{2q}}}_{=:d_k}.$$

The quotient d_k/b_k satisfies

$$\begin{aligned} \frac{d_k}{b_k} &= \frac{t_k^{2q+2r} + \sum_{\nu=1}^{\tau-1} t_{k+n\nu}^{2q+2r}}{\left(t_k^{2q} + \sum_{\nu=1}^{\tau-1} t_{k+n\nu}^{2q} \right) \left(t_k^{2q} - \sum_{\nu=1}^{\tau-1} t_{k+n\nu}^{2q} \right)} \\ &= \frac{t_k^{2q+2r} + \sum_{\nu=1}^{\tau-1} t_{k+n\nu}^{2q+2r}}{t_k^{4q} - \left(\sum_{\nu=1}^{\tau-1} t_{k+n\nu}^{2q} \right)^2}. \end{aligned}$$

If $q \geq r$ then $d_k/b_k > 1$. Hence, if $\tau > 1$, then we have $\text{risk}_q(p = D) < \text{risk}_q(p = n)$. In other words, the lowest risk in the overparameterized regime is strictly less than that in the underparameterized regime. \square

E Proof of Lemmas

E.1 Proof of Lemma 1

Proof of Lemma 1. Using the re-parameterization $\beta = \Sigma^{-q}\theta$, the weighted min-norm estimator is $\hat{\beta}_T := \tilde{\mathbf{F}}_T^\dagger \mathbf{y}, \hat{\beta}_{T^c} := \mathbf{0}$, where $\mathbf{y} = \tilde{\mathbf{F}}_T \beta_T + \tilde{\mathbf{F}}_{T^c} \beta_{T^c}$ and $\tilde{\mathbf{F}} = \mathbf{F} \Sigma^q$.

Since $\tilde{\mathbf{F}}_T$ has full rank the matrix $\tilde{\mathbf{F}}_T \tilde{\mathbf{F}}_T^* = \mathbf{F}_T \Sigma_T^{2q} \mathbf{F}_T^*$ is invertible and $\tilde{\mathbf{F}}_T^\dagger = \tilde{\mathbf{F}}_T^* (\tilde{\mathbf{F}}_T \tilde{\mathbf{F}}_T^*)^{-1}$. The estimation error satisfies

$$\begin{aligned} \|\theta - \hat{\theta}\|_2^2 &= \|\Sigma_T^q (\beta_T - \hat{\beta}_T)\|^2 + \|\Sigma_T^q \Sigma_{T^c} (\beta_{T^c} - \hat{\beta}_{T^c})\|^2 \\ &= \left\| \Sigma_T^q \beta_T - \Sigma_T^q \tilde{\mathbf{F}}_T^\dagger \left(\tilde{\mathbf{F}}_T \beta_T + \tilde{\mathbf{F}}_{T^c} \beta_{T^c} \right) \right\|^2 + \|\Sigma_{T^c}^q \beta_{T^c}\|^2 \\ &= \left\| \Sigma_T^q \left(\mathbf{I} - \tilde{\mathbf{F}}_T^\dagger \tilde{\mathbf{F}}_T \right) \beta_T - \Sigma_T^q \tilde{\mathbf{F}}_T^\dagger \tilde{\mathbf{F}}_{T^c} \beta_{T^c} \right\|^2 + \|\Sigma_{T^c}^q \beta_{T^c}\|^2 \\ &= \left\| \Sigma_T^q \left(\mathbf{I} - \tilde{\mathbf{F}}_T^\dagger \tilde{\mathbf{F}}_T \right) \beta_T \right\|^2 + \left\| \Sigma_T^q \tilde{\mathbf{F}}_T^\dagger \tilde{\mathbf{F}}_{T^c} \beta_{T^c} \right\|^2 + \|\Sigma_{T^c}^q \beta_{T^c}\|^2 \\ &\quad - \underbrace{2 \operatorname{Re} \left(\beta_T^* \left(\mathbf{I} - \tilde{\mathbf{F}}_T^\dagger \tilde{\mathbf{F}}_T \right) \Sigma_T^{2q} \tilde{\mathbf{F}}_T^\dagger \tilde{\mathbf{F}}_{T^c} \beta_{T^c} \right)}_{=: \mathcal{C}_1}. \end{aligned} \tag{20}$$

Since $\tilde{\mathbf{F}}_T^\dagger \tilde{\mathbf{F}}_T$ is Hermitian we have

$$\left\| \Sigma_T^q \left(\mathbf{I} - \tilde{\mathbf{F}}_T^\dagger \tilde{\mathbf{F}}_T \right) \beta_T \right\|^2 = \|\Sigma_T^q \beta_T\|^2 + \left\| \Sigma_T^q \tilde{\mathbf{F}}_T^\dagger \tilde{\mathbf{F}}_T \beta_T \right\|^2 - \underbrace{2 \left(\beta_T^* \Sigma_T^{2q} \tilde{\mathbf{F}}_T^\dagger \tilde{\mathbf{F}}_T \beta_T \right)}_{=: \mathcal{C}_2}. \tag{21}$$

Combining (20) and (21) and taking expectation yields

$$\begin{aligned} \mathbb{E} \left[\|\Sigma^q (\beta - \hat{\beta})\|^2 \right] &= \mathbb{E} \left[\|\Sigma^q \beta\|^2 \right] + \mathbb{E} \left[\left\| \Sigma_T^q \tilde{\mathbf{F}}_T^\dagger \tilde{\mathbf{F}}_T \beta_T \right\|^2 \right] + \mathbb{E} \left[\left\| \Sigma_T^q \tilde{\mathbf{F}}_T^\dagger \tilde{\mathbf{F}}_{T^c} \beta_{T^c} \right\|^2 \right] \\ &\quad - \mathbb{E}[\mathcal{C}_1] - \mathbb{E}[\mathcal{C}_2]. \end{aligned} \tag{22}$$

The "trace trick" and $\tilde{\mathbf{F}}_T^\dagger \tilde{\mathbf{F}}_T = \tilde{\mathbf{F}}_T^* (\tilde{\mathbf{F}}_T \tilde{\mathbf{F}}_T^*)^{-1} \tilde{\mathbf{F}}_T$ give

$$\begin{aligned} \mathbb{E} \left[\left\| \Sigma_T^q \tilde{\mathbf{F}}_T^\dagger \tilde{\mathbf{F}}_T \beta_T \right\|^2 \right] &= \mathbb{E} \left[\text{tr} \left(\beta_T^* \tilde{\mathbf{F}}_T^\dagger \tilde{\mathbf{F}}_T \Sigma_T^q \tilde{\mathbf{F}}_T^\dagger \tilde{\mathbf{F}}_T \beta_T \right) \right] = \text{tr} \left(\tilde{\mathbf{F}}_T^\dagger \tilde{\mathbf{F}}_T \Sigma_T^{2q} \tilde{\mathbf{F}}_T^\dagger \tilde{\mathbf{F}}_T \mathbb{E}[\beta_T \beta_T^*] \right) \\ &= \text{tr} \left(\Sigma_T^{2q} \tilde{\mathbf{F}}_T^\dagger \tilde{\mathbf{F}}_T \Sigma_T^{-q} \mathbf{K}_T \Sigma_T^{-q} \right) = \text{tr} \left(\tilde{\mathbf{F}}_T \mathbf{K}_T \tilde{\mathbf{F}}_T^* (\tilde{\mathbf{F}}_T \tilde{\mathbf{F}}_T^*)^{-1} \right) = \text{tr} \left((\mathbf{K}_T) \tilde{\mathbf{F}}_T^\dagger \tilde{\mathbf{F}}_T \right). \end{aligned}$$

Moreover,

$$\begin{aligned} \mathbb{E} \left[\left\| \Sigma_T^q \tilde{\mathbf{F}}_T^\dagger \tilde{\mathbf{F}}_T \beta_{T^c} \right\|^2 \right] &= \text{tr} \left(\tilde{\mathbf{F}}_{T^c}^* (\tilde{\mathbf{F}}_T^\dagger)^* \Sigma_T^{2q} \tilde{\mathbf{F}}_T^\dagger \tilde{\mathbf{F}}_{T^c} \mathbb{E}[\beta_{T^c} \beta_{T^c}^*] \right) \\ &= \text{tr} \left(\Sigma_T^{2q} \tilde{\mathbf{F}}_T^\dagger \tilde{\mathbf{F}}_{T^c} \Sigma_{T^c}^{-q} \mathbf{K}_{T^c} \Sigma_{T^c}^{-q} \right) \tilde{\mathbf{F}}_{T^c}^* (\tilde{\mathbf{F}}_T^\dagger)^* \\ &= \text{tr} \left(\Sigma_T^{2q} \tilde{\mathbf{F}}_T^* (\tilde{\mathbf{F}}_T \tilde{\mathbf{F}}_T^*)^{-1} \mathbf{F}_{T^c} \mathbf{K}_{T^c} \mathbf{F}_{T^c}^* (\tilde{\mathbf{F}}_T \tilde{\mathbf{F}}_T^*)^{-1} \tilde{\mathbf{F}}_T \right). \end{aligned}$$

Since $\mathbb{E}[\beta_{T^c} \beta_{T^c}^*] = \Sigma_{T^c}^{-q} \mathbb{E}[\mathbf{x}_{T^c} \mathbf{x}_{T^c}^*] \Sigma_{T^c}^{-q} = 0$ we have $\mathbb{E}[\mathcal{C}_1] = 0$. Furthermore, since \mathbf{K} commutes with Σ^{-q} by diagonality, we have $\Sigma_T^{2q} \mathbb{E}[\beta_T \beta_T^*] = \Sigma_T^{2q} \mathbb{E}[\Sigma^{-q} \boldsymbol{\theta} \boldsymbol{\theta}^* \Sigma^{-q}] = \mathbf{K}$ so that

$$\mathbb{E}[\mathcal{C}_2] = 2 \text{tr} \left(\tilde{\mathbf{F}}_T^\dagger \tilde{\mathbf{F}}_T \Sigma_T^{2q} \mathbb{E}[\beta_T \beta_T^*] \right) = 2 \text{tr} \left(\mathbf{K}_T \tilde{\mathbf{F}}_T^\dagger \tilde{\mathbf{F}}_T \right).$$

Plugging all the terms into (22), we have

$$\begin{aligned} \text{risk}_q &= \mathbb{E} \left[\left\| \Sigma^q (\beta - \hat{\beta}) \right\|^2 \right] = \text{tr}(\mathbf{K}) - \text{tr} \left(\mathbf{F}_T \Sigma_T^{2q} \mathbf{K}_T \mathbf{F}_T^* (\mathbf{F}_T \Sigma_T^{2q} \mathbf{F}_T^*)^{-1} \right) \\ &\quad + \text{tr} \left(\mathbf{F}_T \Sigma_T^{4q} \mathbf{F}_T^* (\mathbf{F}_T \Sigma_T^{2q} \mathbf{F}_T^*)^{-1} \mathbf{F}_{T^c} \mathbf{K}_{T^c} \mathbf{F}_{T^c}^* (\mathbf{F}_T \Sigma_T^{2q} \mathbf{F}_T^*)^{-1} \right). \end{aligned}$$

The risk of the plain min-norm estimator corresponds to $q = 0$, which gives

$$\begin{aligned} \text{risk}_0 &= \mathbb{E} \left[\|\boldsymbol{\theta} - \hat{\boldsymbol{\theta}}\|^2 \right] \\ &= \text{tr}(\mathbf{K}) - \text{tr} \left(\mathbf{F}_T \mathbf{K}_T \mathbf{F}_T^* (\mathbf{F}_T \mathbf{F}_T^*)^{-1} \right) + \text{tr} \left(\mathbf{F}_{T^c} \mathbf{K}_{T^c} \mathbf{F}_{T^c}^* (\mathbf{F}_T \mathbf{F}_T^*)^{-1} \right). \quad \square \end{aligned}$$

E.2 Proof of Lemma 2

Proof of Lemma 2. For $u \geq 0$, we set $\mathbf{A}_u = \mathbf{F}_T \Sigma_T^u \mathbf{F}_T^*$ and $\mathbf{C}_u = \mathbf{F}_{T^c} \Sigma_{T^c}^u \mathbf{F}_{T^c}^*$, and define $\omega_n = \exp(-\frac{2\pi i}{n})$. Since $p = nl$, we have, for $j_1, j_2 \in [n]$,

$$\begin{aligned} (\mathbf{A}_u)_{j_1, j_2} &= (\mathbf{F}_T \Sigma_T^u \mathbf{F}_T^*)_{j_1, j_2} = \sum_{k=0}^{p-1} t_k^u \exp \left(\frac{-2\pi i}{n} (j_2 - j_1) \cdot k \right) = \sum_{\nu=0}^{l-1} \sum_{k=0}^{n-1} t_{k+n\nu}^u \omega_n^{(j_2-j_1)k}, \\ (\mathbf{C}_u)_{j_1, j_2} &= (\mathbf{F}_{T^c} \Sigma_{T^c}^u \mathbf{F}_{T^c}^*)_{j_1, j_2} = \sum_{k=p}^{D-1} t_k^u \exp \left(\frac{-2\pi i}{n} (j_2 - j_1) \cdot k \right) = \sum_{\nu=l}^{\tau-1} \sum_{k=0}^{n-1} t_{k+n\nu}^u \omega_n^{(j_2-j_1)k}. \end{aligned}$$

In the above equations, we use $\omega_n^{k+n\nu} = \omega_n^k$ for $\nu \in \mathbb{N}_+$.

For $j \in [n]$, let $a_j = \sum_{\nu=0}^{l-1} \sum_{k=0}^{n-1} t_{k+n\nu}^u \omega_n^{-jk}$ and $c_j = \sum_{\nu=l}^{\tau-1} \sum_{k=0}^{n-1} t_{k+n\nu}^u \omega_n^{-jk}$. Then

$$\begin{aligned} (\mathbf{A}_u)_{j_1, j_2} &= \sum_{\nu=0}^{l-1} \sum_{k=0}^{n-1} t_{k+n\nu}^u \omega_n^{(j_2-j_1)k} = a_{j_2-j_1} \pmod{n}, \\ (\mathbf{C}_u)_{j_1, j_2} &= \sum_{\nu=l}^{\tau-1} \sum_{k=0}^{n-1} t_{k+n\nu}^u \omega_n^{(j_2-j_1)k} = c_{j_2-j_1} \pmod{n}. \end{aligned} \tag{23}$$

Hence, for any $u \geq 0$, \mathbf{A}_u and \mathbf{C}_u are circulant matrices.

For $u = 0$ we use again $p = nl$, $l \in \mathbb{N}_+$ to obtain that, for $j_1, j_2 \in [n]$,

$$(\mathbf{F}_T \mathbf{F}_T^*)_{j_1, j_2} = \sum_{k=0}^{p-1} \omega_n^{(j_2-j_1)k} = \begin{cases} p, & \text{if } j_1 = j_2, \\ 0, & \text{if } j_1 \neq j_2. \end{cases}$$

Hence, $\mathbf{F}_T \mathbf{F}_T^* = p \mathbf{I}_n$ as claimed. \square

E.3 Proof of Lemma 4

Proof of Lemma 4. In the under-parameterized setting, the error of the least square estimator satisfies

$$\begin{aligned}\|\boldsymbol{\theta} - \hat{\boldsymbol{\theta}}\|^2 &= \|(\mathbf{F}_T^* \mathbf{F}_T)^{-1} \mathbf{F}_T^* (\mathbf{F}_T \mathbf{x}_T + \mathbf{F}_{T^c} \mathbf{x}_{T^c}) - \mathbf{x}_T\|^2 + \|\mathbf{x}_{T^c}\|^2 \\ &= \|(\mathbf{F}_T^* \mathbf{F}_T)^{-1} \mathbf{F}_T^* \mathbf{F}_{T^c} \mathbf{x}_{T^c}\|^2 + \|\mathbf{x}_{T^c}\|^2 \\ &= \text{tr}(\mathbf{F}_{T^c}^* \mathbf{F}_T (\mathbf{F}_T^* \mathbf{F}_T)^{-2} \mathbf{F}_T^* \mathbf{F}_{T^c} \mathbf{x}_{T^c} \mathbf{x}_{T^c}^*) + \|\mathbf{x}_{T^c}\|^2.\end{aligned}$$

Taking expectation yields

$$\mathbb{E}[\|\boldsymbol{\theta} - \hat{\boldsymbol{\theta}}\|^2] = c_r \text{tr}(\Sigma_{T^c}^{2r}) + c_r \text{tr}(\mathbf{F}_T (\mathbf{F}_T^* \mathbf{F}_T)^{-2} \mathbf{F}_T^* \mathbf{F}_{T^c} \Sigma_{T^c}^{2r} \mathbf{F}_{T^c}^*).$$

□

F Visualization of Theoretical Risks

F.1 Heat Maps of Theoretical Risks

We show the heat maps of the theoretical risks of weighted and plain min-norm estimators in Figure 6, which are calculated by Theorem 1 and 3. Here, we use Fourier series models with $D = 1024$, varying n , and $q = r$. The x-axis is r of the r -decaying coefficients (r is from 0 to 2 with 0.1 as the step), the y-axis is p (where $p < n$ in the underparameterized regime and $p = ln, l \in \mathbb{N}_+$ in the overparameterized regime), and the risks are in log scale. We can see the trends of the risks: the left three plots in Figure 6 show that when $q = r > 1$ the risk monotonically decreases as p increases in the underparameterized regime and the lowest risk lies in the overparameterized regime; while the right three plots show that after $p > n$, the risks of plain min-norm estimator ($q = 0$) increase suddenly and they are higher (i.e., the light color block in each heat map⁹) than the risks in then underparameterized regime when $r > 1$. Hence, these plots also verify Theorem 4.

F.2 Theoretical Risks with varying r and q

Figures 7 and 8 show the plots of the theoretical extended risk curves (fixed n) with a range of choices for r and q as mentioned in Remark 4.1, from which we can see all the trends and patterns of the risks. In this experiment, we use Fourier series models with $D = 1024$, n varying from 8 to 1024, $p < n$ in the underparameterized regime and $p = ln, l \in \mathbb{N}_+$ in the overparameterized regime. We investigate on $r = 0, 0.3, 0.5, 0.7, 1.0, 1.5, 2.0, 3.0$ and p with the same range but not necessarily equal to r (the curves with $q = 0$ correspond to the risks of the plain min-norm estimator).

Some observations of the plots are as follows.

1. For varying n , the trends with the same r and q are similar along with different transition points ($p = n$), except for the case $r = 0$ and $n \geq D/2$ (as it states in Remark 3.1, when $n < D/2$, the risk increases with p in the underparameterized regime while for $n \geq D/2$ it goes to the other direction.)
2. In the underparameterized regime, when $r = 0$ and $n < D/2$, the risk increases with p until $p = n$. This behavior of the risk curve persists a while, then transitions to a U -shape curve, and then transitions to a decreasing curve, as we vary r in the range $0 \leq r \leq 1$. For $r \geq 1$, the risk is monotonically decreasing in p (as we proved in Theorem 4).
3. In the overparameterized regime, the risk of the plain min-norm estimator is almost above the weighted min-norm estimator when $r \geq 0.5$. Even if the weight matrix we use does not match the covariance matrix exactly for r -decaying coefficients, the weighted min-norm estimator usually achieves lower risks than the plain min-norm estimator.
4. As it is stated in the proof of Theorem 4 (Appendix D), the plots also show that when $q \geq r$, the risk at $p = D$ is strictly lower than that at $p = n$, and $r \geq 1$ is a sufficient condition to assure the monotonic decrease when $p < n$ and the lowest risk in the overparameterized regime is strictly lower than that in the underparameterized regime.

⁹Note that these heat maps on the right are not corrupted.

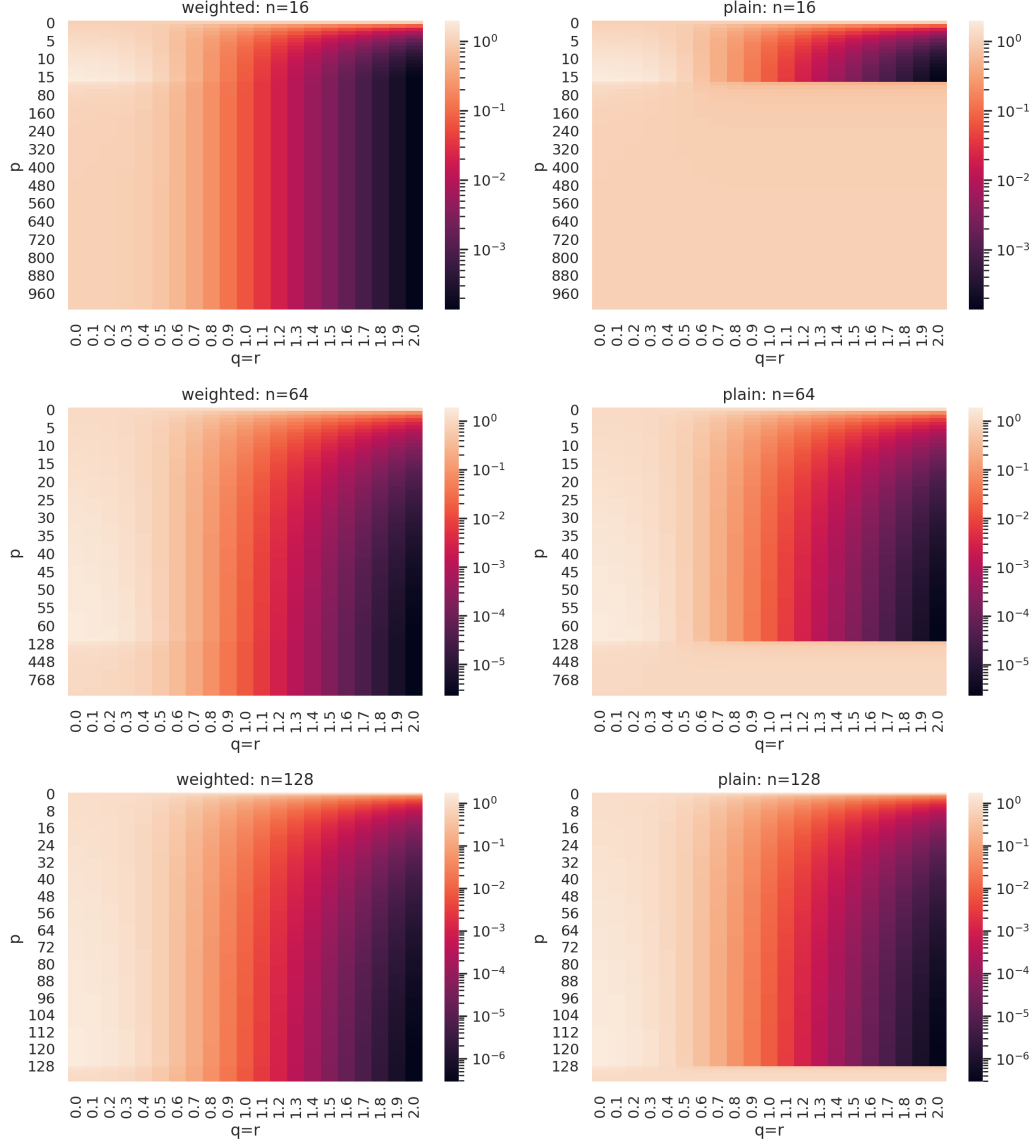


Figure 6: Heat maps of theoretical risks of weighted (left) and plain min-norm (right) estimators of r -decaying features. $D = 1024$, $q = r$, and $n = 16, 64, 128$. (Note the these heat maps on the right are not corrupted: there are light color blocks since the risks of the plain min-norm estimators (i.e., $q = 0$ in Figure 7) changes to around 1 after $p > n$, and the color bar is in log scale. This transition also occurs with the weighted estimator, where the faint horizontal line takes place ($p = n$). It corresponds to a peak in risk, as illustrated in Figure 7.)

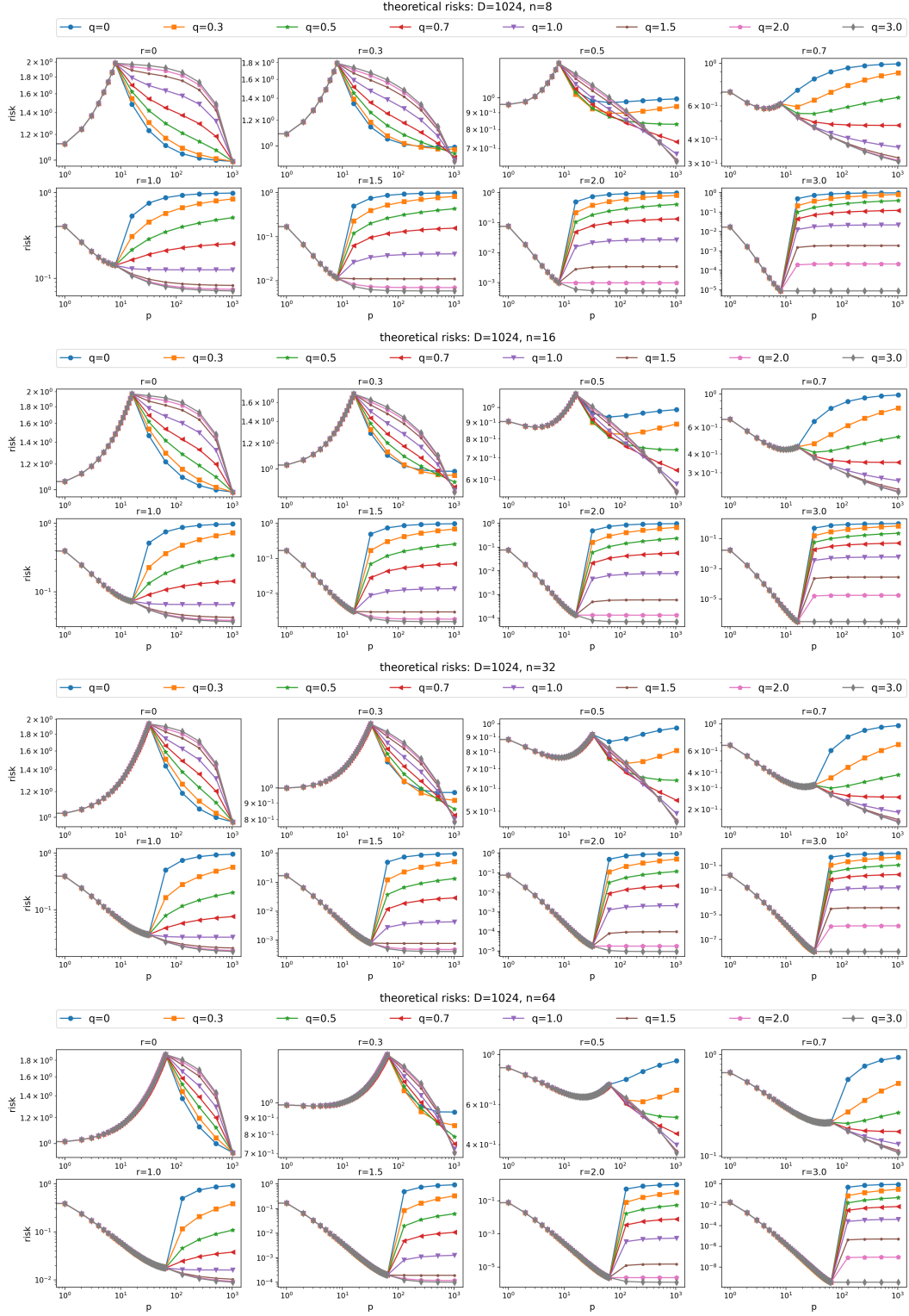


Figure 7: Theoretical risks of r -decaying features and varying q with $D = 1024$, where plain min-norm estimator corresponds to $q = 0$. From top to bottom: $n = 8, 16, 32, 64$.

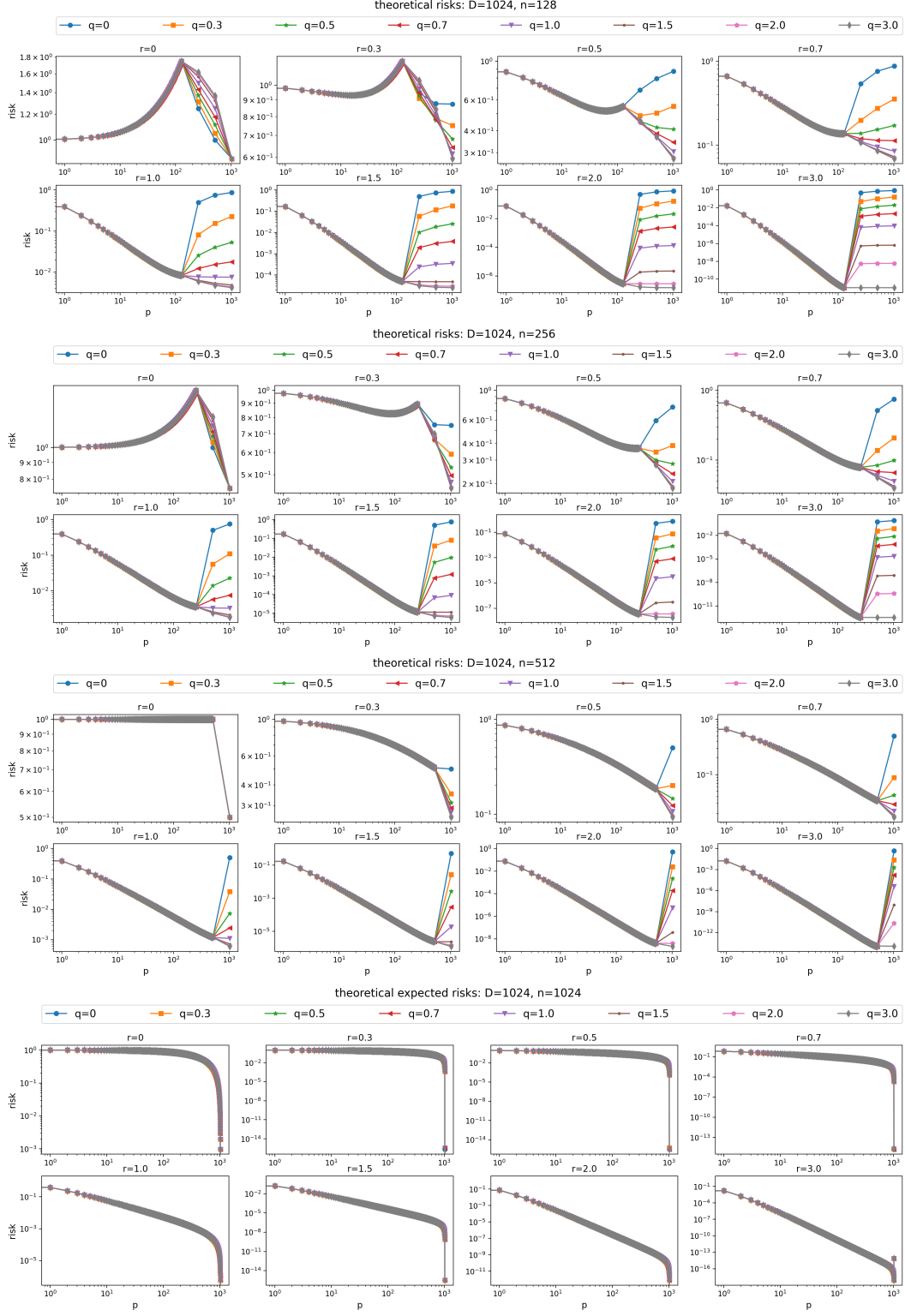


Figure 8: Theoretical risks of r -decaying features and varying q with $D = 1024$, where plain min-norm estimator corresponds to $q = 0$. From top to bottom: $n = 128, 256, 512, 1024$.